Electronic Supplementary Material (ESI) for Organic & Biomolecular Chemistry.
This journal is © The Royal Society of Chemistry 2018

Electronic Supplementary Information1

Dihydroindeno[1,2-*b*]pyrroles: New Al^{3+} selective off-on chemosensors for bio-imaging in living HepG2 cell

Kajal Mal,[a] Barnali Naskar,[a] Animesh Mondal,[a] Sanchita Goswami,[a] Chandraday Prodhan,[b] Keya Chaudhuri[b] and Chhanda Mukhopadhyay *[a]

*E-mail: cmukhop@yahoo.co.in

Contents of the Supporting Information

Contents of the Supporting Information	Pages
addition of EDTA. ……………………………………………………………………………………..	32
Figure S41. Fluorescence emission spectra of chemosensor (**6j**) in the presence of Al^{3+} ion followed by addition of EDTA. …………………………………………………………………………………	32
Figure S42. Emission intensity of compounds **4a, 4e, 4g, 4h, 6g and 6j** in absence and in presence of Al^{3+} at different pH values in aqueous DMSO solution. ………………………………………………..	33-35
Figure S43. Anion independency of emission intensity of **4a and 4e** in presence of various Al^{3+} salts [e.g. $Al(ClO_4)_3$, $AlCl_3$ and $Al(NO_3)_3$]…………………………………………………………………………	36
Figure S44. Anion independency of emission intensity of **4g and 4h** in presence of various Al^{3+} salts [e.g. $Al(ClO_4)_3$, $AlCl_3$ and $Al(NO_3)_3$]…………………………………………………………………………	37
Figure S45. Anion independency of emission intensity of **6j** in presence of various Al^{3+} salts [e.g. $Al(ClO_4)_3$, $AlCl_3$ and $Al(NO_3)_3$]…………………………………………………………………………	38
Figure S46. Excitation spectra of **4a** and **4e** in presence of Al^{3+} in solution………………………………..	39
Figure S47. Excitation spectra of **4g** and **4h** in presence of Al^{3+} in solution…………………………….	40
Figure S48. Excitation spectra of **6g** and **6j** in presence of Al^{3+} in solution……………………………	41
Figure S49. ^{1}H NMR titration of chemosensor **6j** with Al^{3+} metal ion in DMSO-d_6...................................	42
Table S4. Summary of photophysical properties of compounds **4a, 4e, 4g, 4h, 6g and 6j** studied in various solvents...	43-45
Table S5. Stability constant (*K*) and Limit of detection studied with complexation properties of the compounds (**4a, 4e, 4g, 4h, 6g** and **6j**)..	45
Table S6. Comparison with recently reported probes for selective detection of Al^{3+} ion………………..	46-49

1. Characterization, Structure and Crystallographic Data

Electrospray ionization mass spectra: (HR–ESI–MS) were recorded on Qtof Micro YA263 mass spectrometer dissolving the samples in LC–MS quality methanol.
Figure S1. ESI–MS spectra of compound **4a, 4e, 4g, 4h, 6g, 6j** and in Aluminium complexes.

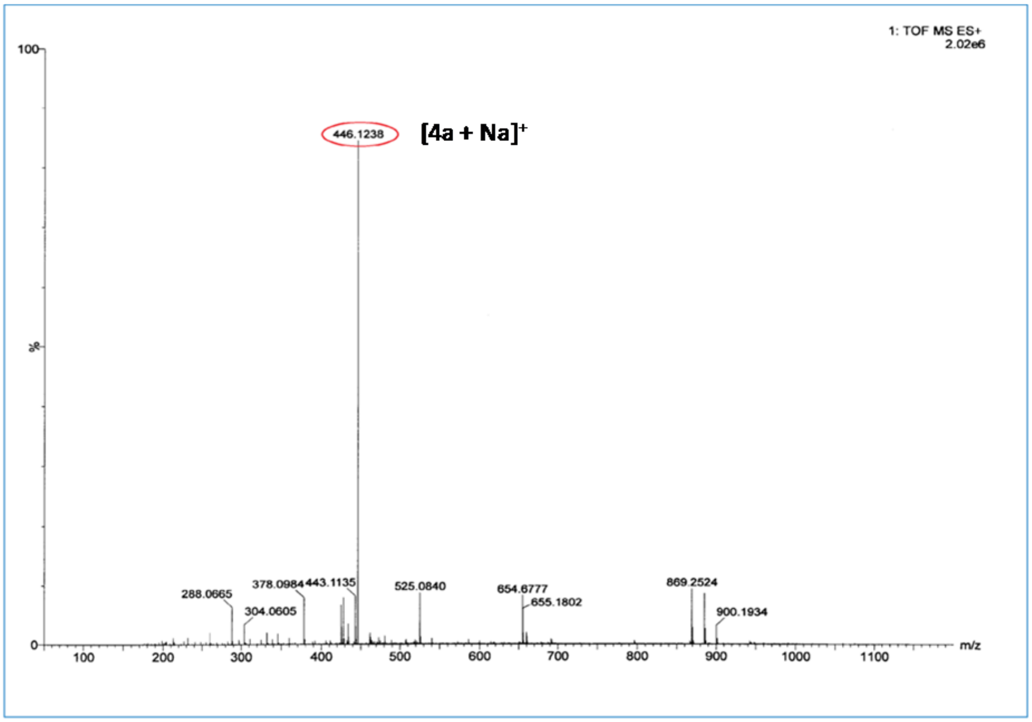

ESI-MS of compound **4a**

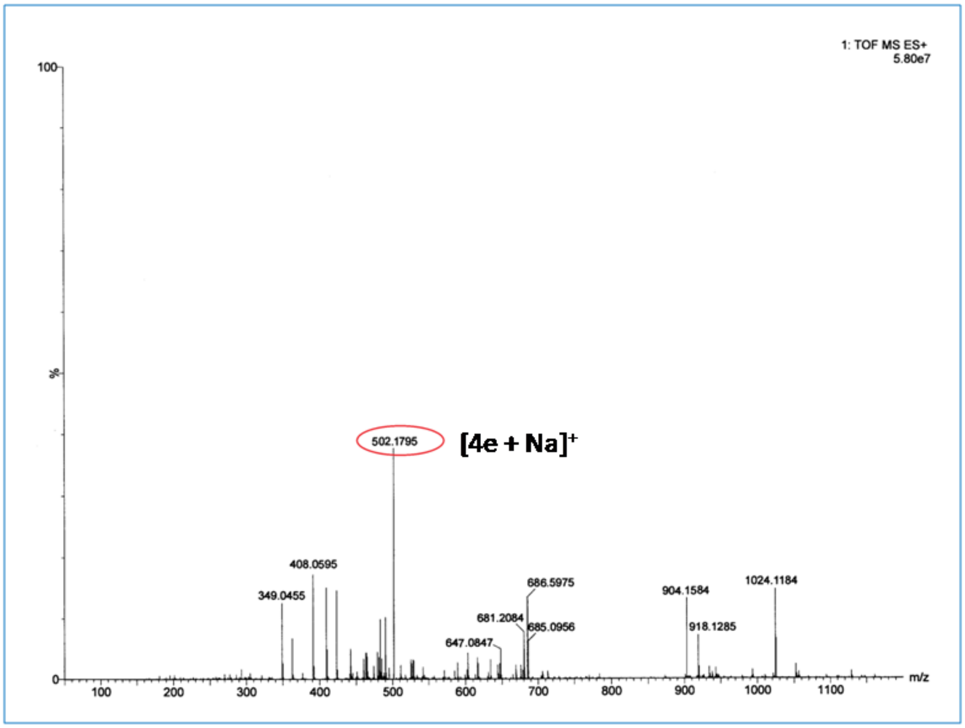

ESI-MS of compound **4e**

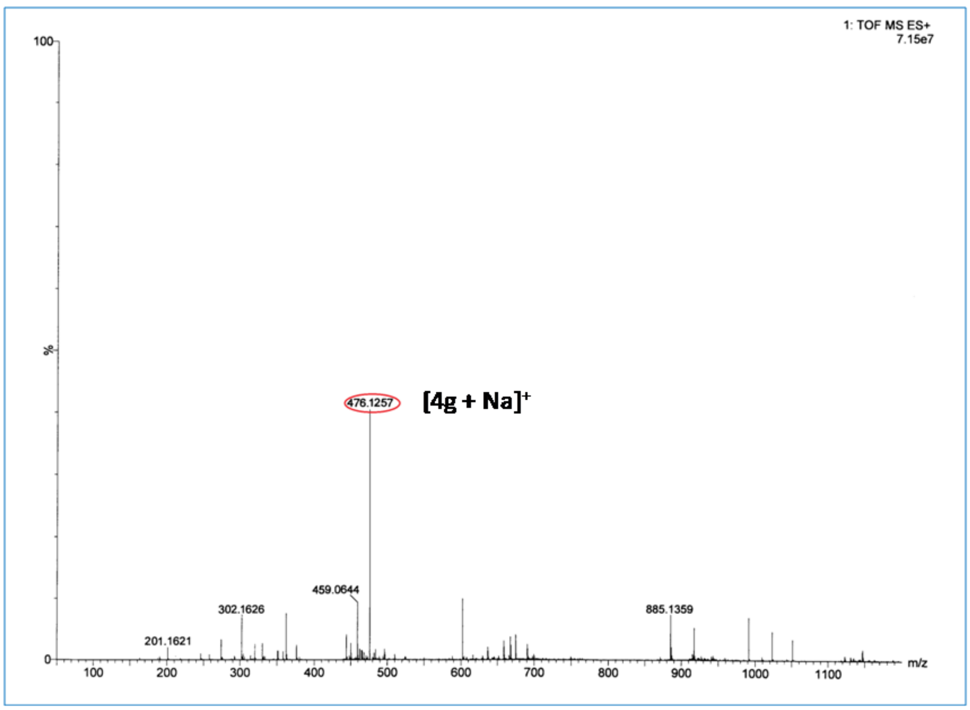

ESI-MS of compound **4g**

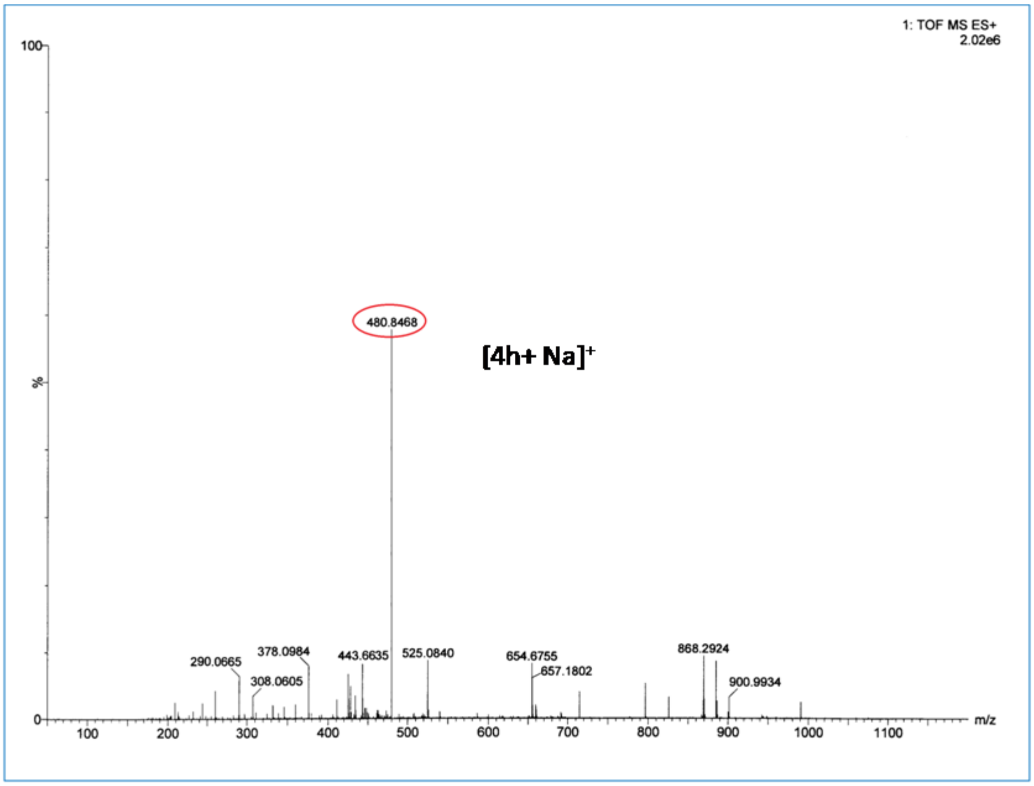

ESI-MS of compound **4h**

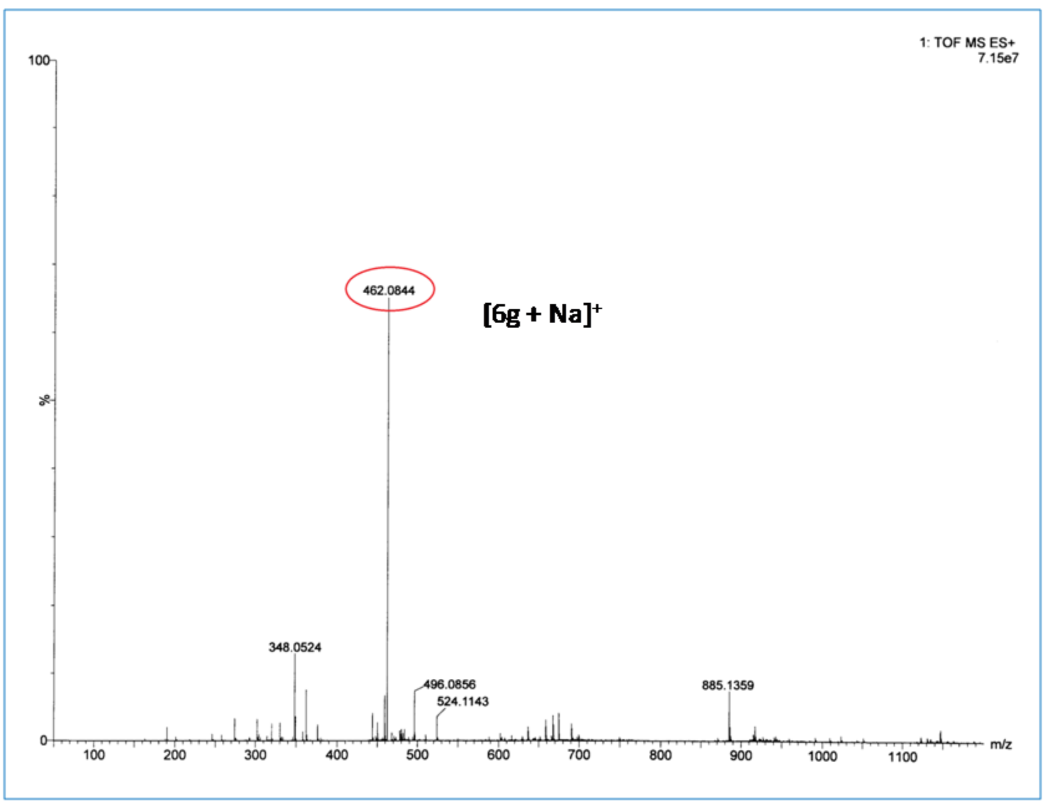

ESI-MS of compound **6g**

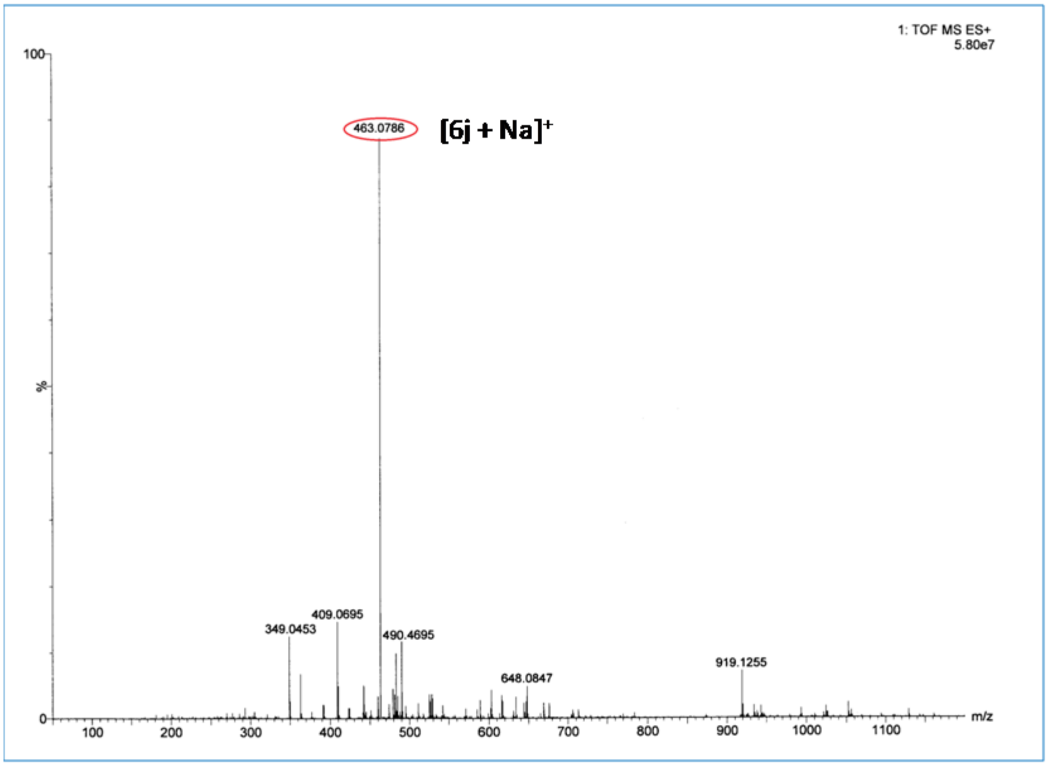

ESI-MS of compound**6j**

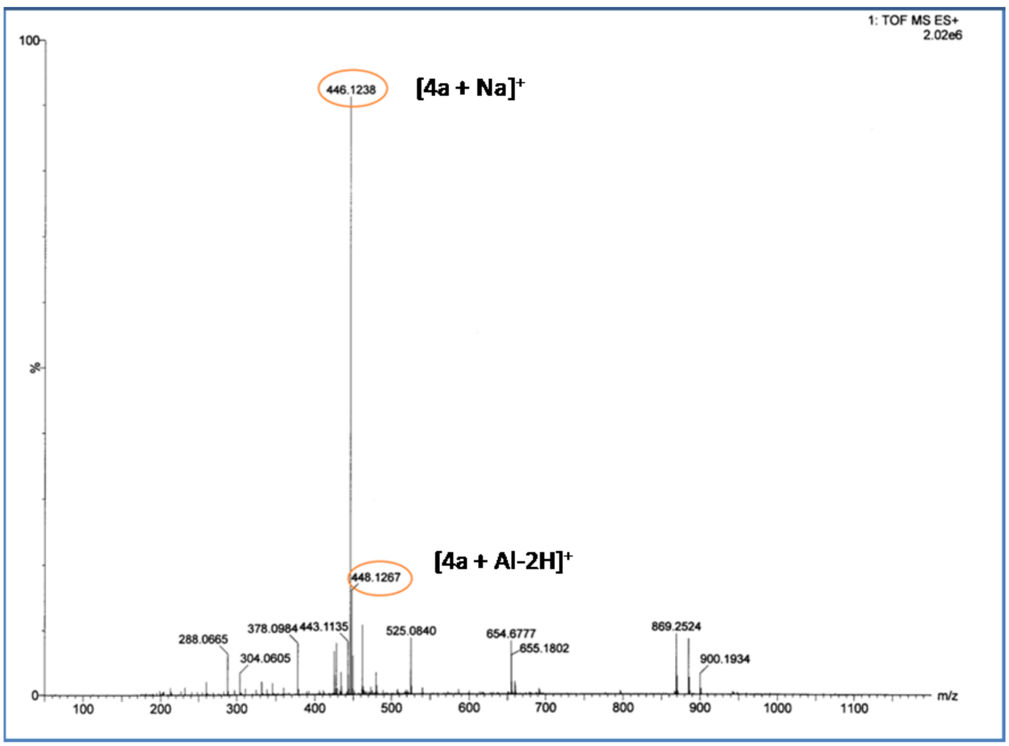

ESI-MS of compound **4a+Al**

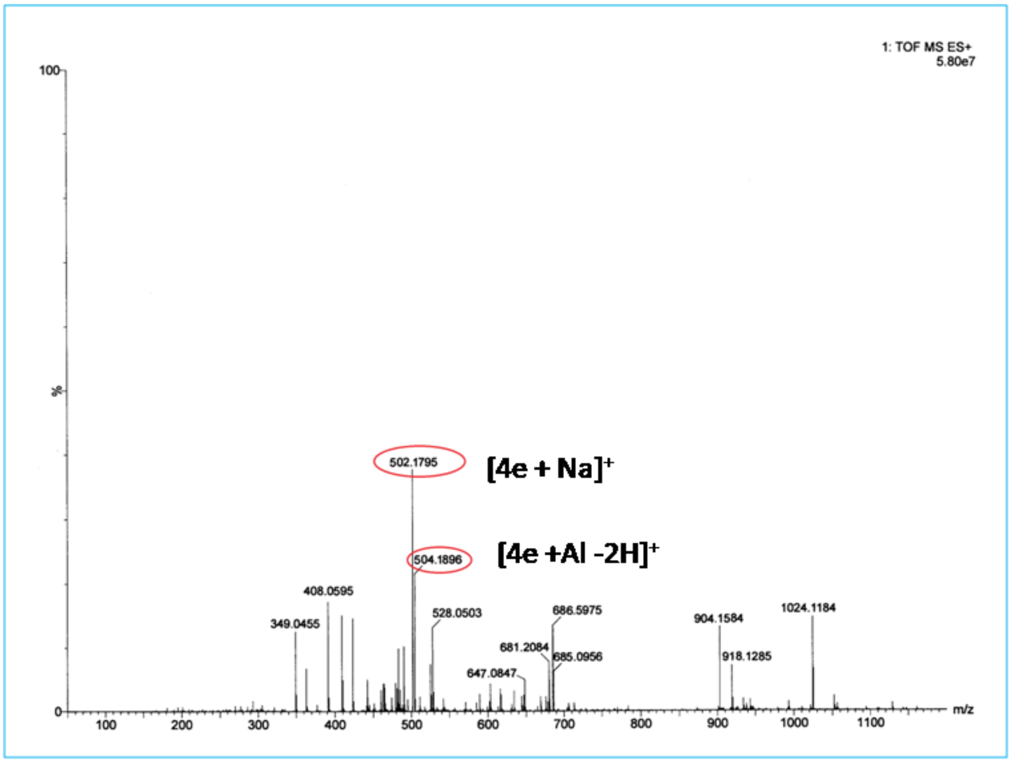

ESI-MS of compound **4e+Al**

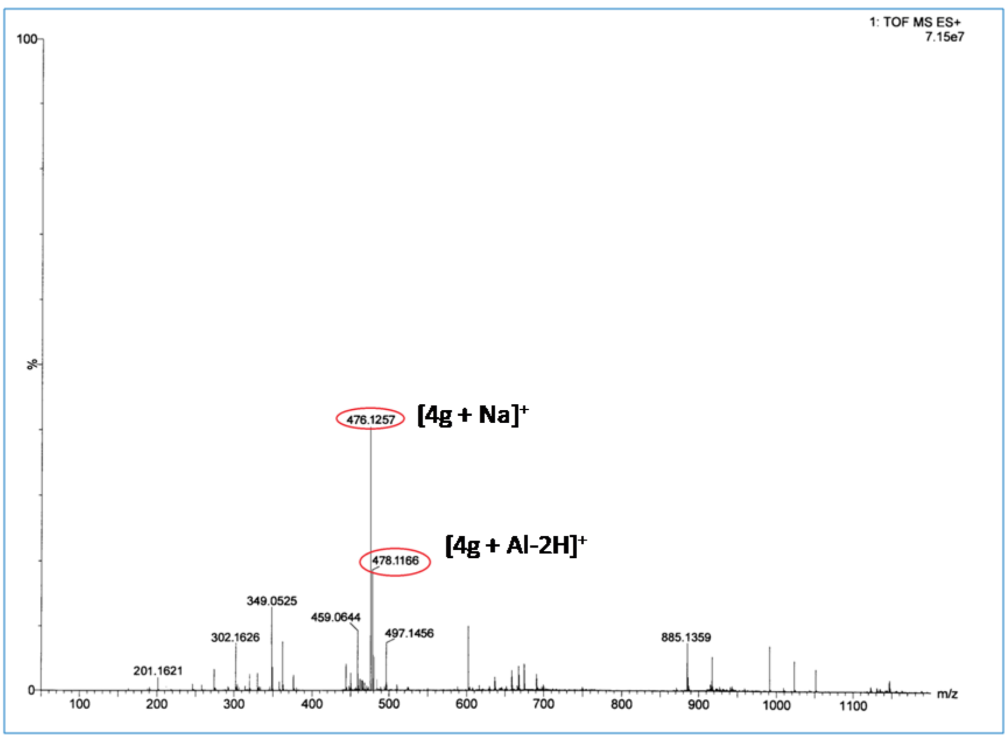

ESI-MS of compound **4g+Al**

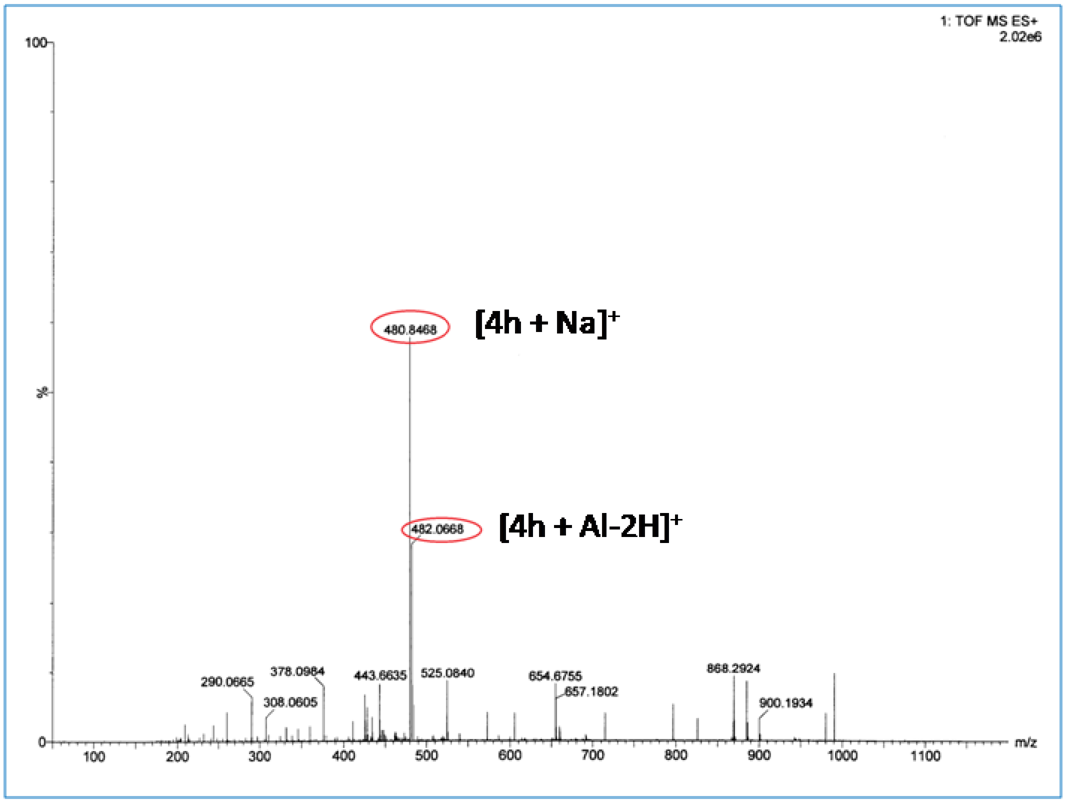

ESI-MS of compound **4h+Al**

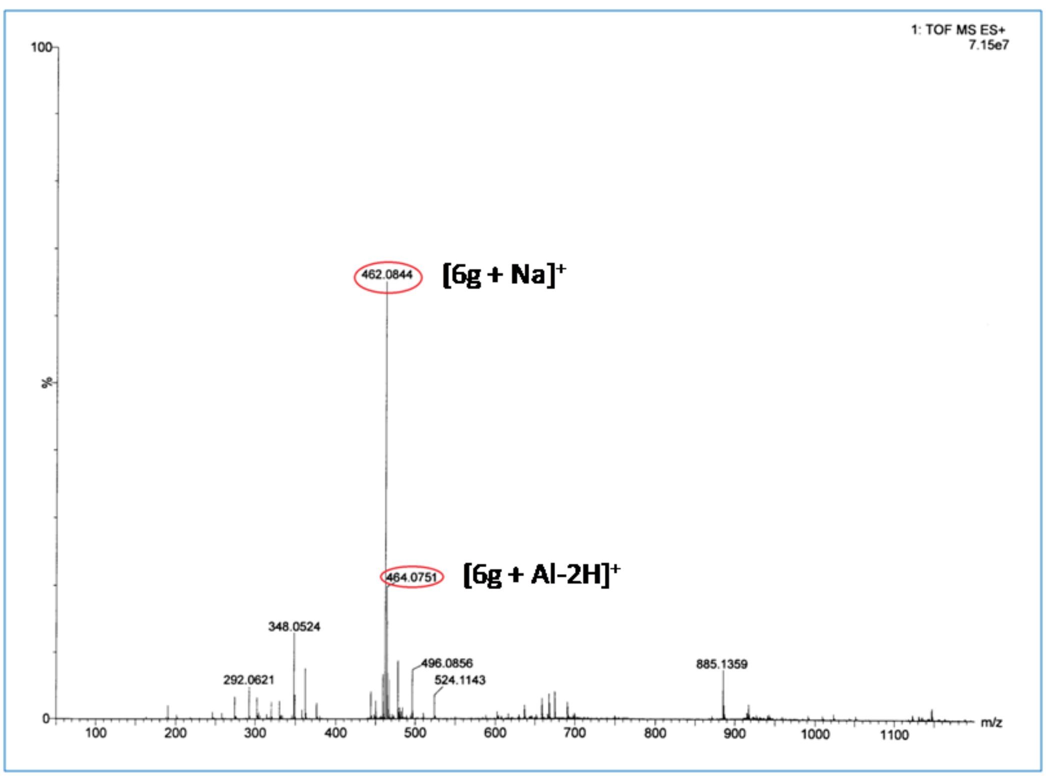

ESI-MS of compound **6g+Al**

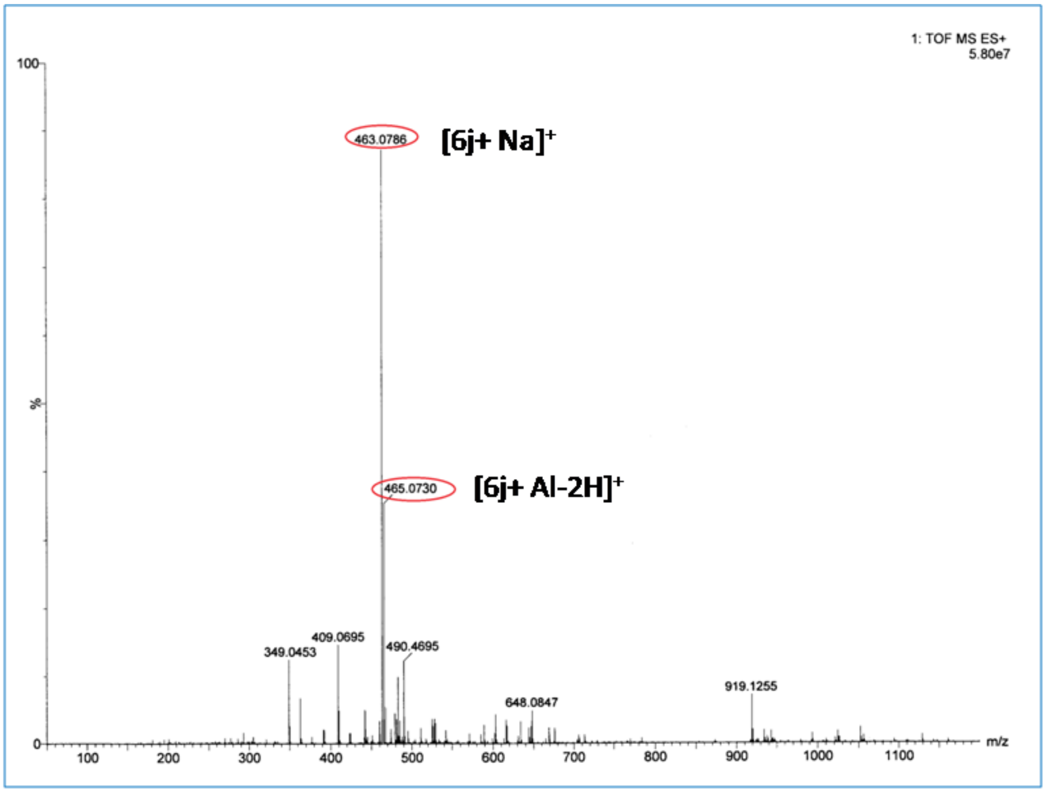

ESI-MS of compound **6j+Al**

2. Photophysical Characterization

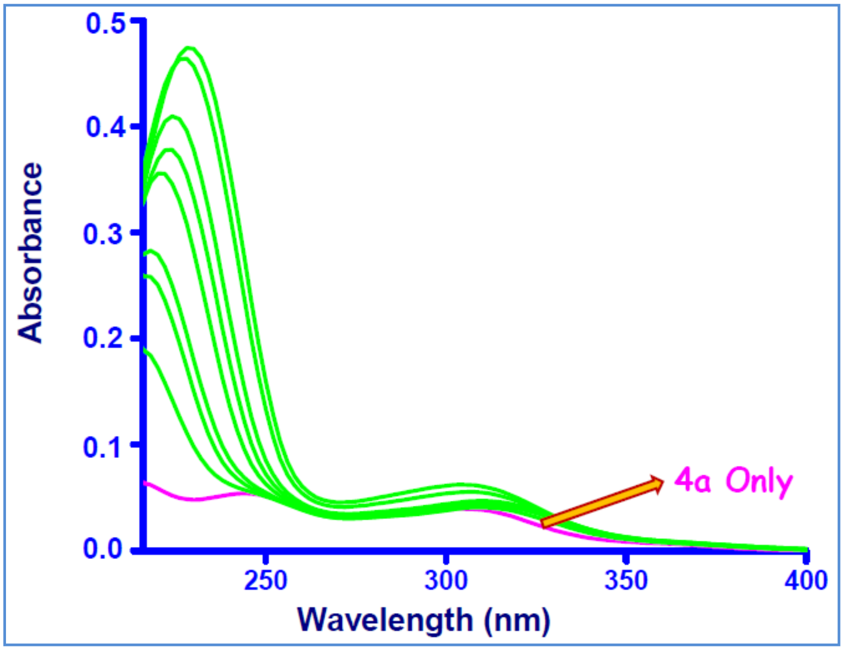

Figure S2. UV-vis spectra of **4a** (5×10^{-6} M) in DMSO/H_2O (2 : 8, v/v) HEPES buffer (pH = 7.4) solution in the presence of various concentrations of Al^{3+} (0, 1, 2, 3, 4, 5, 6, 8 and 10) $\times10^{-6}$ M.

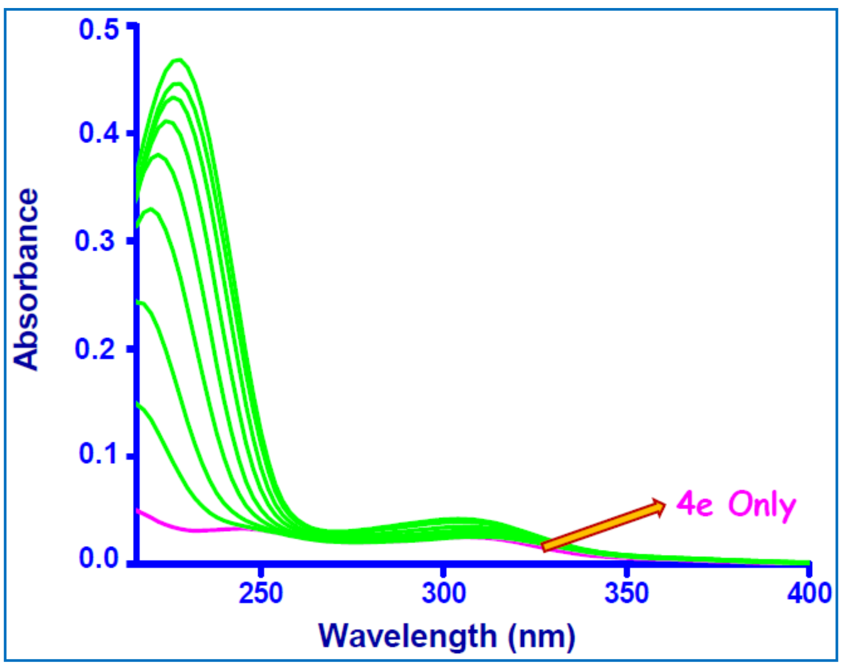

Figure S3. UV-vis spectra of **4e** (5×10^{-6} M) in DMSO/H_2O (2 : 8, v/v) HEPES buffer (pH = 7.4) solution in the presence of various concentrations of Al^{3+} (0, 1, 2, 3, 4, 5, 6, 8 and 10) $\times10^{-6}$ M.

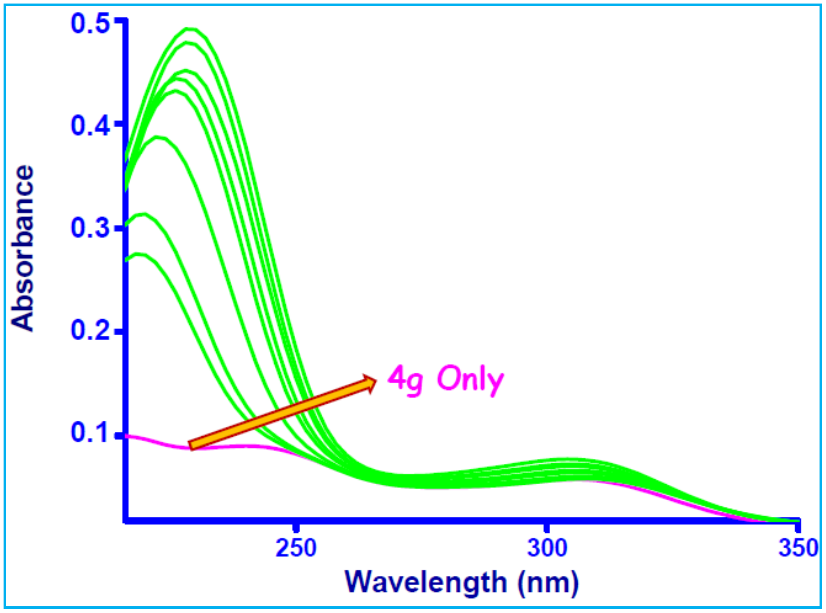

Figure S4. UV-vis spectra of **4g** (5×10^{-6} M) in DMSO/H_2O (2 : 8, v/v) HEPES buffer (pH = 7.4) solution in the presence of various concentrations of Al^{3+} (0, 1, 2, 3, 4, 5, 6, 8 and 10) $\times10^{-6}$ M.

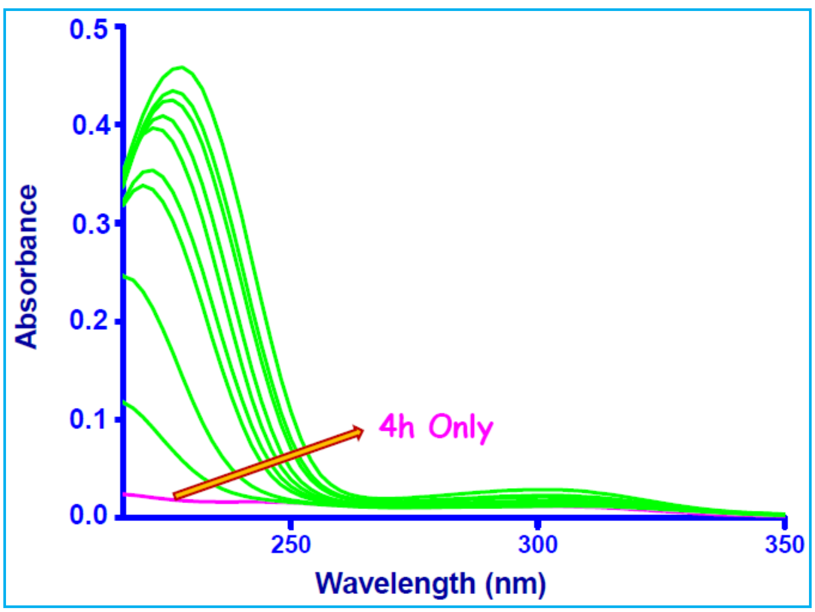

Figure S5. UV-vis spectra of **4h** (5×10^{-6} M) in DMSO/H_2O (2 : 8, v/v) HEPES buffer (pH = 7.4) solution in the presence of various concentrations of Al^{3+} (0, 1, 2, 3, 4, 5, 6, 7, 8 and 10) $\times10^{-6}$ M.

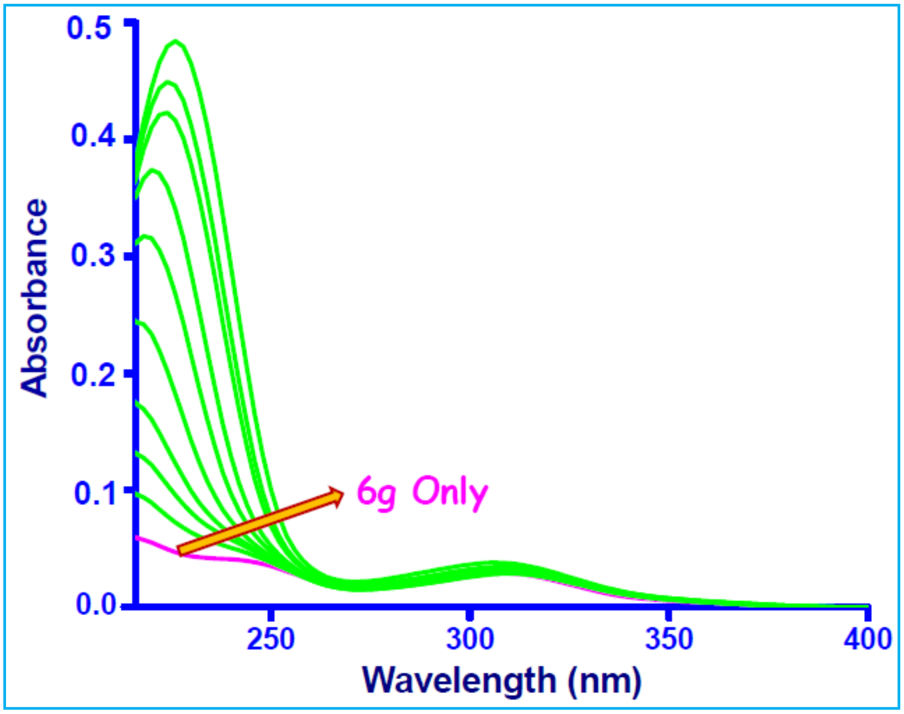

Figure S6. UV-vis spectra of **6g** (5×10^{-6} M) in DMSO/H_2O (2 : 8, v/v) HEPES buffer (pH = 7.4) solution in the presence of various concentrations of Al^{3+} (0, 1, 2, 3, 4, 5, 6, 7, 8 and 10) $\times10^{-6}$ M.

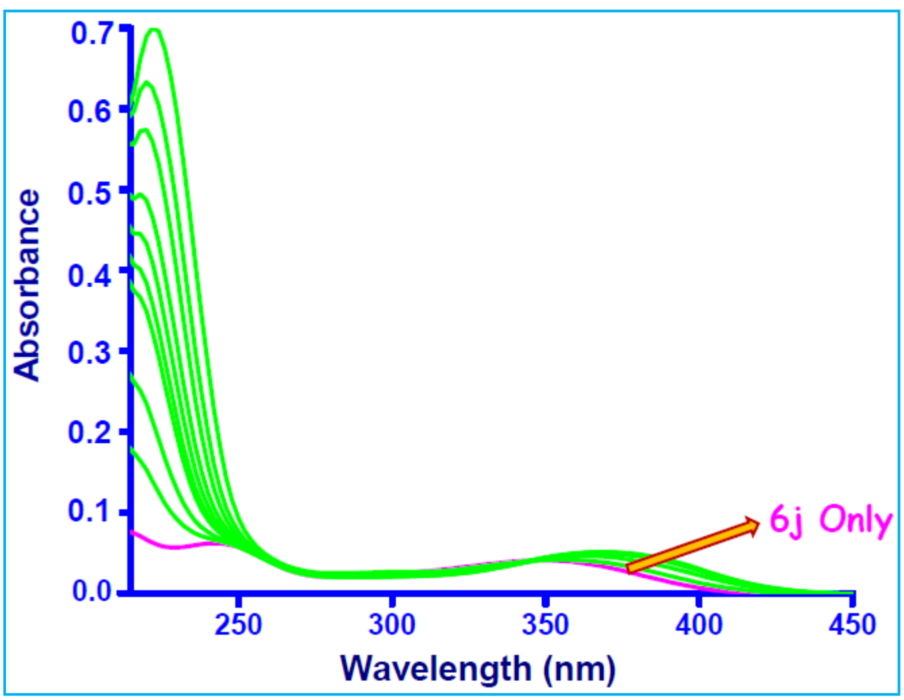

Figure S7. UV-vis spectra of **6j** (5×10^{-6} M) in DMSO/H_2O (2 : 8, v/v) HEPES buffer (pH = 7.4) solution in the presence of various concentrations of Al^{3+} (0, 1, 2, 3, 4, 5, 6, 7, 8 and 10) $\times10^{-6}$ M.

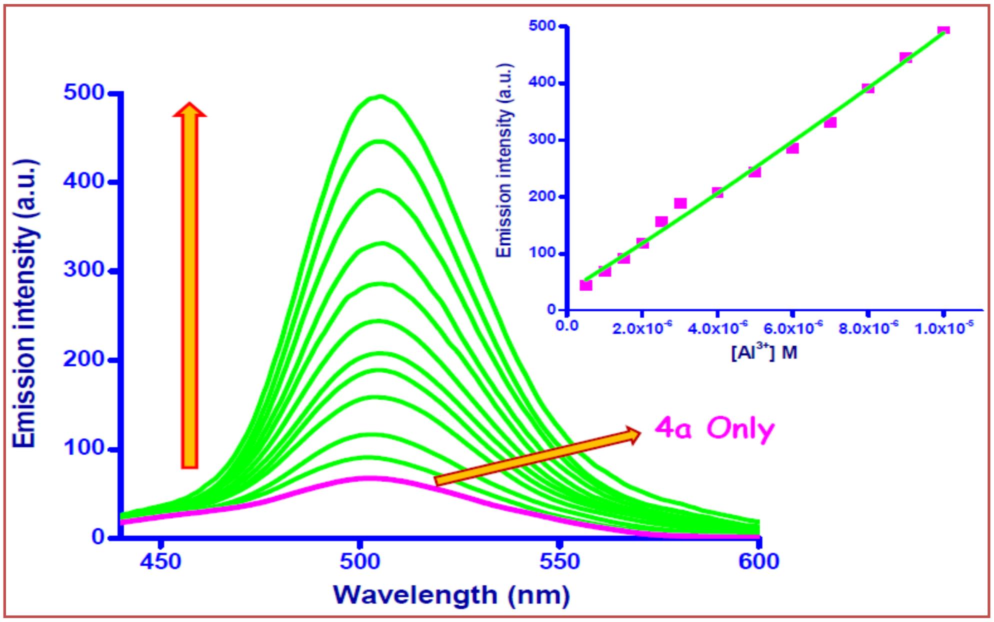

Figure S8. Emission spectra of **4a** (5×10^{-6} M) in the presence of increasing amounts of [Al^{3+}] (0, 0.5, 1, 2, 3, 4, 5, 6, 7, 8, 9 and 10 ($\times 10^{-6}$) M in DMSO/H_2O (2 : 8, v/v) HEPES buffer (pH = 7.4) solution (λ_{ex} = 310.33 nm, λ_{em} = 504.90 nm). Inset: Fluorescence emission intensity of **4a** at 504.90 nm as a function of [Al^{3+}].

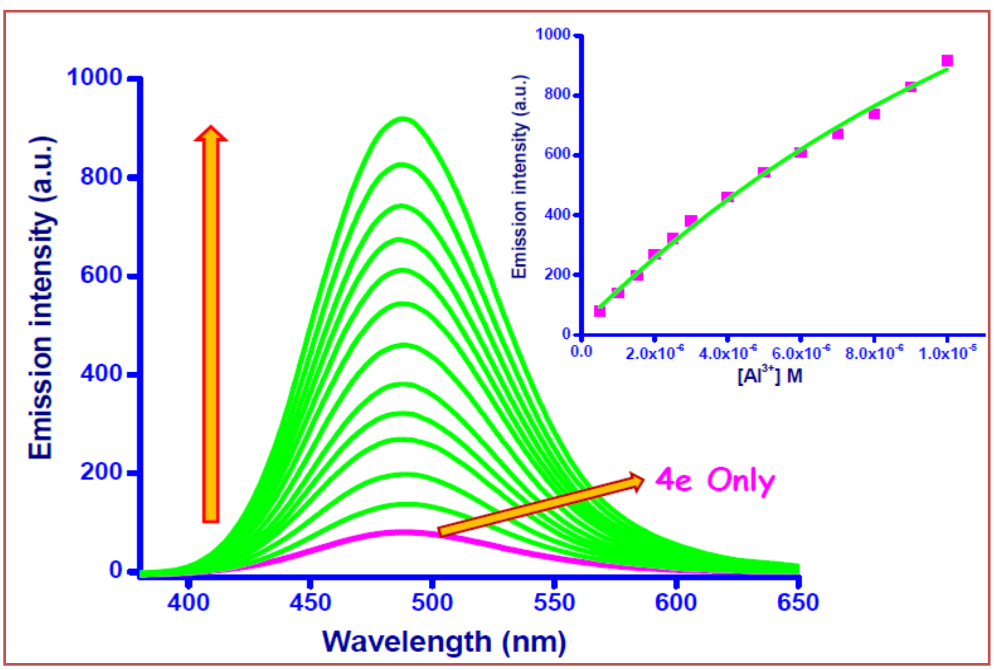

Figure S9. Emission spectra of **4e** (5×10^{-6} M) in the presence of increasing amounts of [Al^{3+}] (0, 0.5, 1, 1.5, 2, 3, 4, 5, 6, 7, 8, 9 and 10 ($\times 10^{-6}$) M in DMSO/H_2O (2 : 8, v/v)

HEPES buffer (pH = 7.4) solution (λ_{ex} = 308.69 nm, λ_{em} = 489.25 nm). Inset: Fluorescence emission intensity of 4e at 489.25 nm as a function of [Al^{3+}].

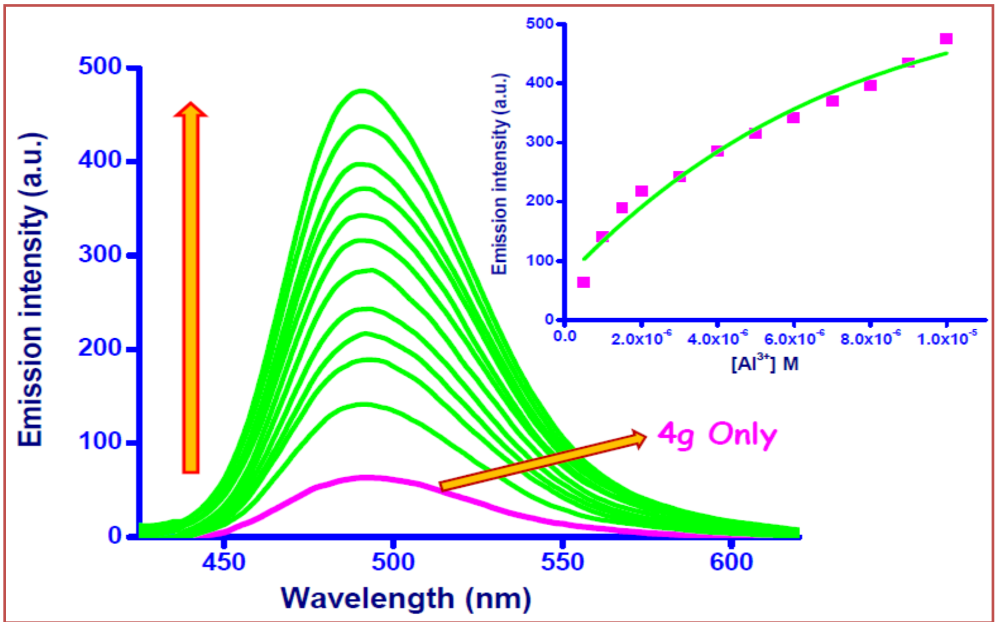

Figure S10. Emission spectra of **4g** (5×10^{-6} M) in the presence of increasing amounts of [Al^{3+}] (0, 0.5, 1, 2, 3, 4, 5, 6, 7, 8, 9 and 10 ($\times 10^{-6}$) M in DMSO/H_2O (2 : 8, v/v) HEPES buffer (pH = 7.4) solution (λ_{ex} = 308.97 nm, λ_{em} = 491.22 nm). Inset: Fluorescence emission intensity of 4g at 491.22 nm as a function of [Al^{3+}].

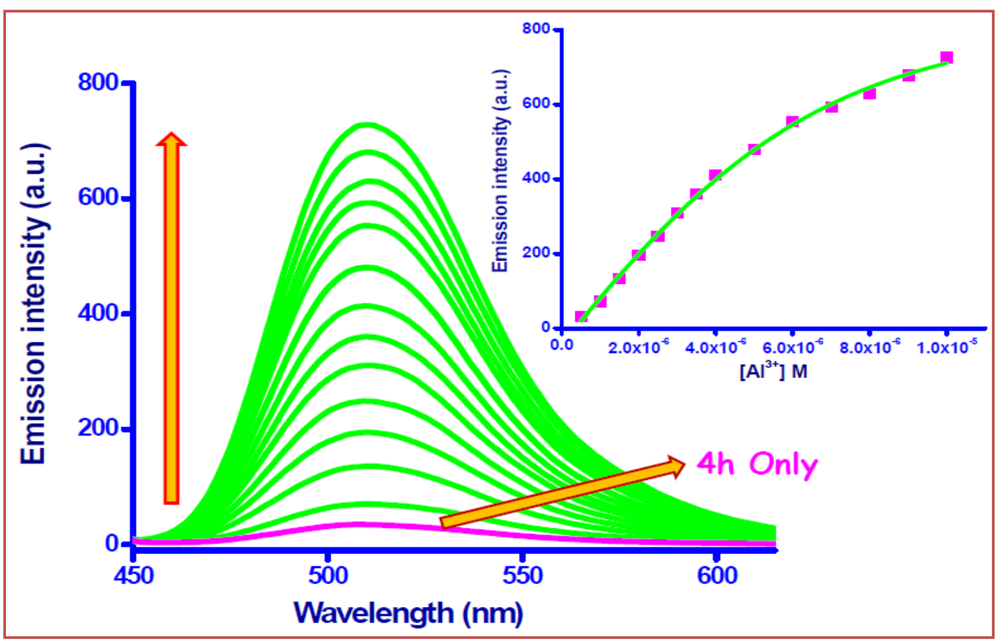

Figure S11. Emission spectra of **4h** (5×10^{-6} M) in the presence of increasing amounts of [Al^{3+}] (0, 0.5, 1, 1.5, 2, 2.5, 3, 4, 5, 6, 7, 8, 9 and 10 ($\times 10^{-6}$) M in DMSO/H_2O (2 : 8, v/v)

HEPES buffer (pH = 7.4) solution (λ_{ex} = 305.82 nm, λ_{em} = 505.31 nm). Inset: Fluorescence emission intensity of 4h at 505.31 nm as a function of [Al^{3+}].

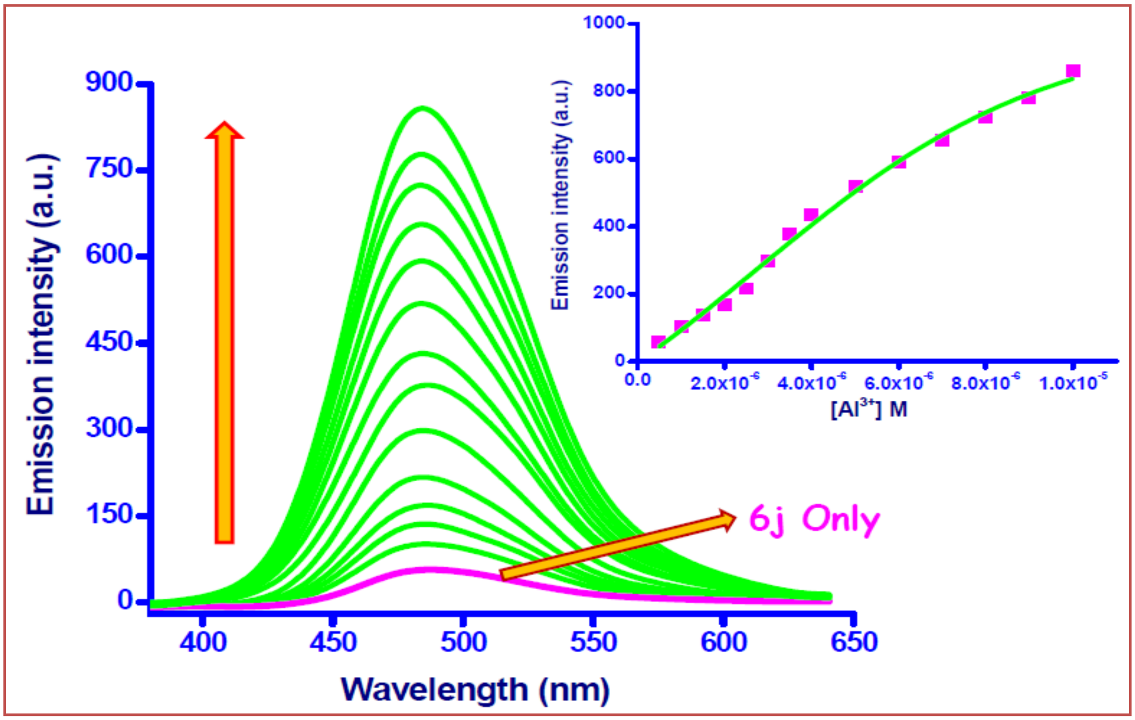

Figure S12. Emission spectra of **6j** (5 × 10^{-6} M) in the presence of increasing amounts of [Al^{3+}] (0, 0.5, 1, 1.5, 2, 2.5, 3, 4, 5, 6, 7, 8, 9 and 10 (×10^{-6}) M in DMSO/H_2O (2 : 8, v/v) HEPES buffer (pH = 7.4) solution (λ_{ex} = 320.11 nm, λ_{em} = 485.65 nm). Inset: Fluorescence emission intensity of 6j at 485.65 nm as a function of [Al^{3+}].

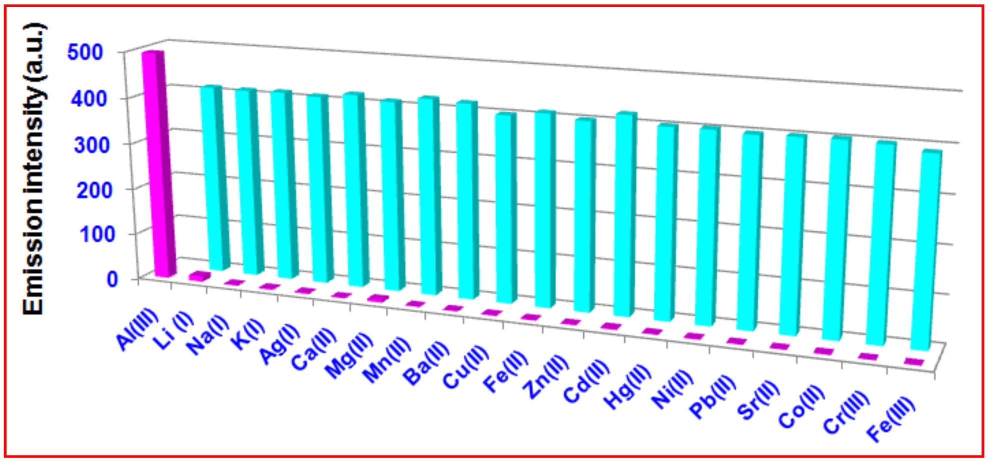

Figure S13. Fluorescence emission spectra of **4a** (5×10^{-6} M) in the presence of 4 equiv. of different cations except 2 equiv. of Al^{3+} in solution [the majenta bar portion]. Fluorescence intensity of a mixture of **4a** (5×10^{-6} M) with other metal ions (20×10^{-6} M) followed by addition of Al^{3+} (10×10^{-6} M) to the HEPES buffer (pH = 7.4) solution [the cyan bar portion] (λ_{ex} = 310.33 nm, λ_{em} = 504.90 nm).

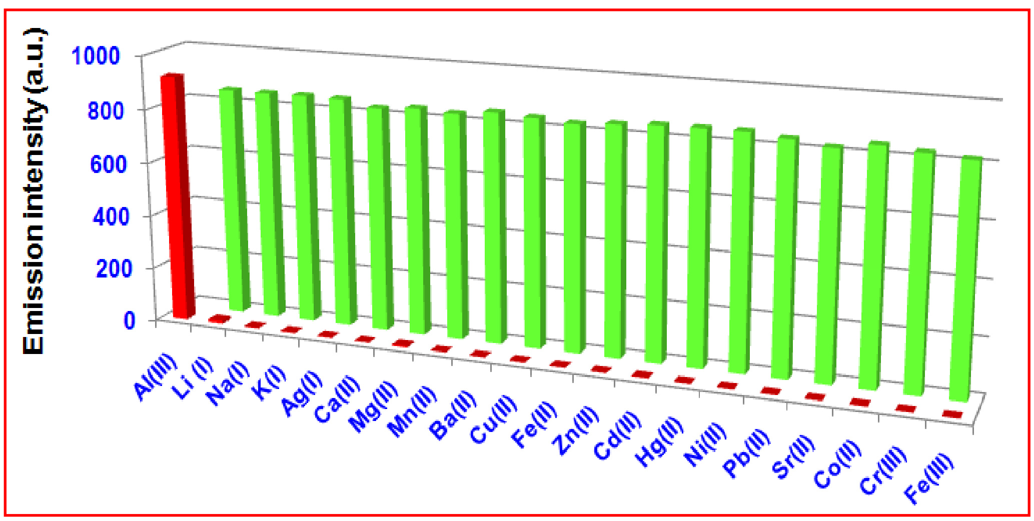

Figure S14. Fluorescence emission spectra of **4e** (5×10^{-6} M) in the presence of 4 equiv. of different cations except 2 equiv. of Al^{3+} in solution [the red bar portion]. Fluorescence intensity of a mixture of 4e (5×10^{-6} M) with other metal ions (20×10^{-6} M) followed by addition of Al^{3+} (10×10^{-6} M) to the HEPES buffer (pH = 7.4) solution [the green bar portion] (λ_{ex} = 308.69 nm, λ_{em} = 489.25 nm).

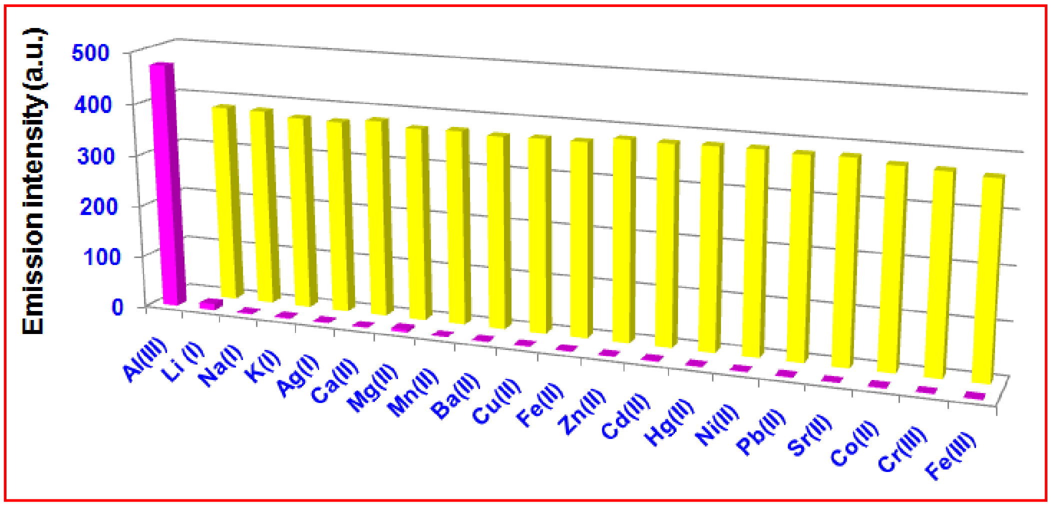

Figure S15. Fluorescence emission spectra of **4g** (5×10^{-6} M) in the presence of 4 equiv. of different cations except 2 equiv. of Al^{3+} in solution [the majenta bar portion]. Fluorescence intensity of a mixture of 4g (5×10^{-6} M) with other metal ions (20×10^{-6} M) followed by addition of Al^{3+} (10×10^{-6} M) to the HEPES buffer (pH = 7.4) solution [the yellow bar portion] (λ_{ex} = 308.97 nm, λ_{em} = 491.22 nm).

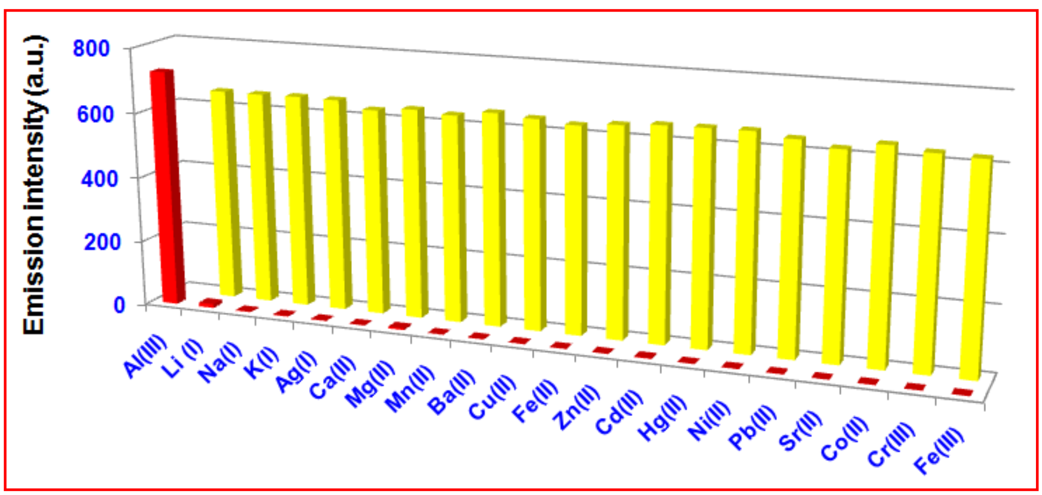

Figure S16. Fluorescence emission spectra of **4h** (5×10^{-6} M) in the presence of 4 equiv. of different cations except 2 equiv. of Al^{3+} in solution [the red bar portion]. Fluorescence intensity of a mixture of 4h (5×10^{-6} M) with other metal ions (20×10^{-6} M) followed by addition of Al^{3+} (10×10^{-6} M) to the HEPES buffer (pH = 7.4) solution [the yellow bar portion] (λ_{ex} = 305.82 nm, λ_{em} = 505.31 nm).

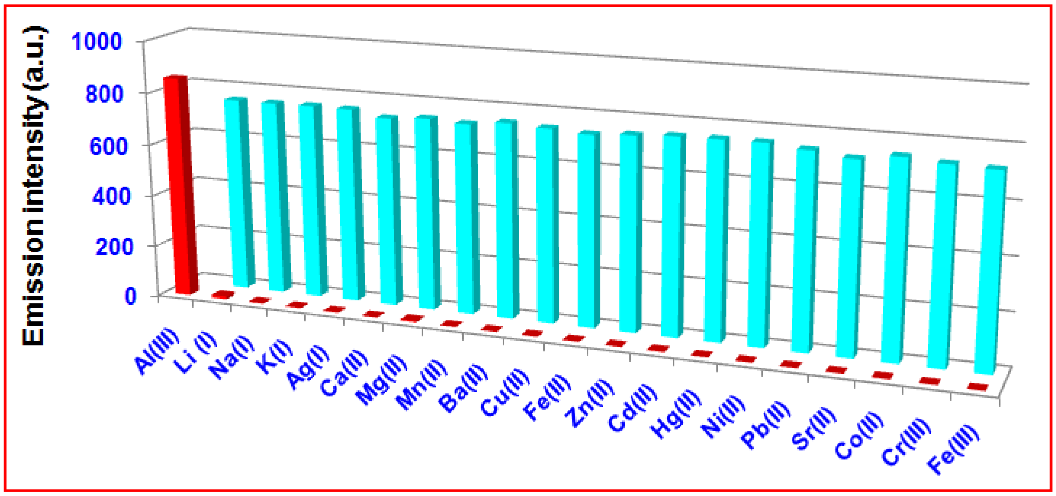

Figure S17. Fluorescence emission spectra of **6j** (5×10^{-6} M) in the presence of 4 equiv. of different cations except 2 equiv. of Al^{3+} in solution [the red bar portion]. Fluorescence intensity of a mixture of **6j** (5×10^{-6} M) with other metal ions (20×10^{-6} M) followed by addition of Al^{3+} (10×10^{-6} M) to the HEPES buffer (pH = 7.4) solution [the cyan bar portion] (λ_{ex} = 320.11 nm, λ_{em} = 485.65 nm)

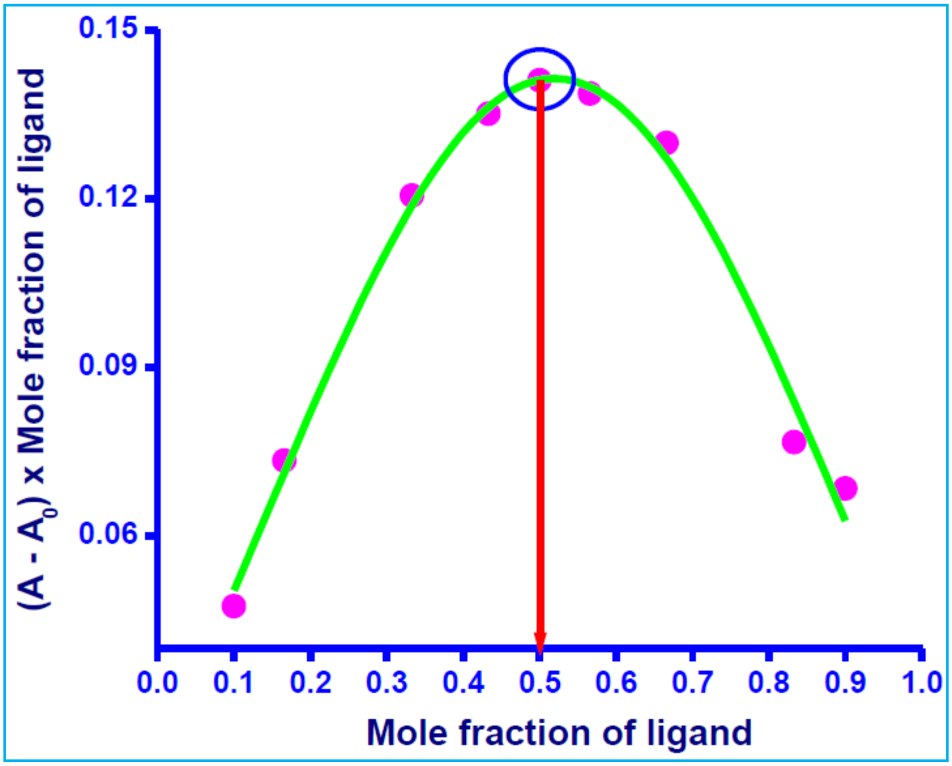

Figure S18. Job′s plot for determination of stoichiometry of Al^{3+} : **4a** complex in solution.

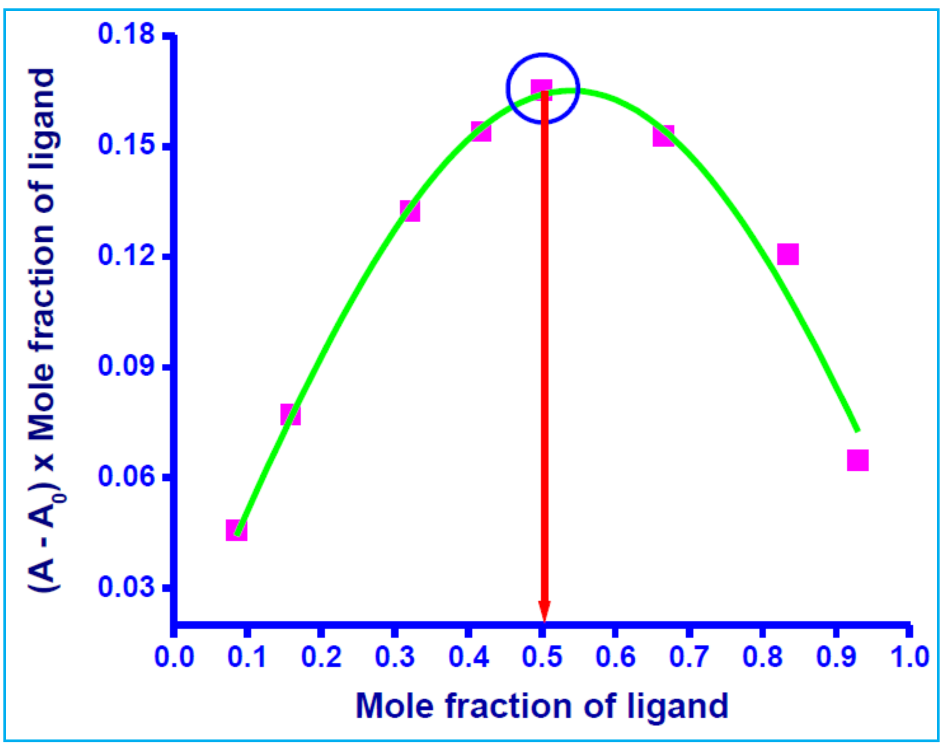

Figure S19. Job′s plot for determination of stoichiometry of Al^{3+} : **4e** complex in solution.

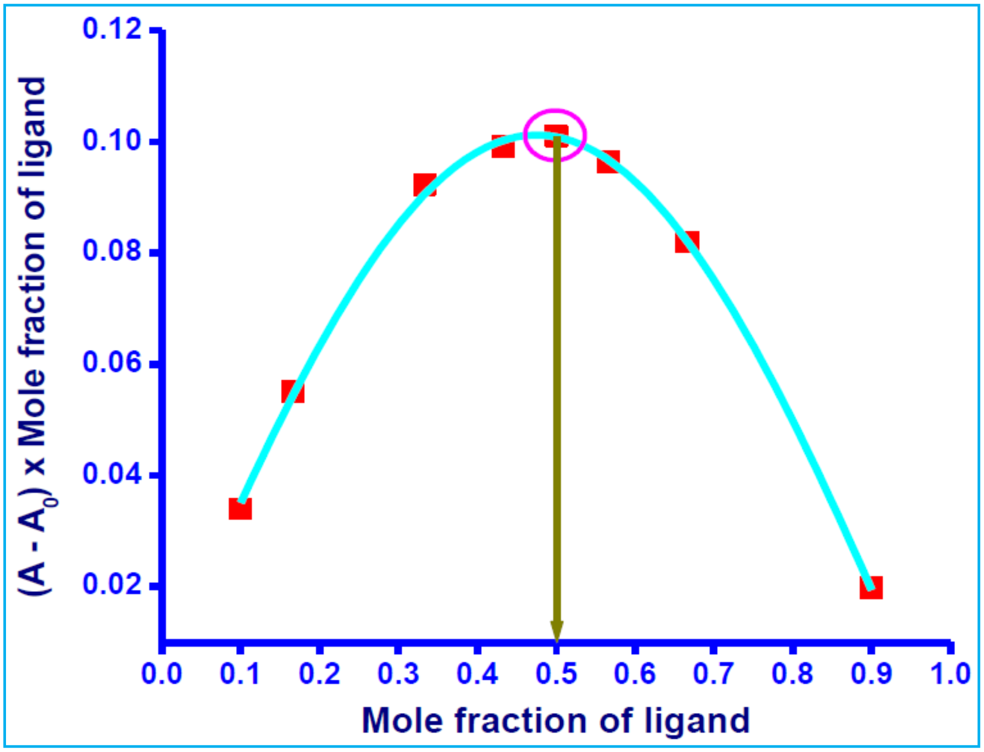

Figure S20. Job's plot for determination of stoichiometry of Al^{3+} : **4g** complex in solution.

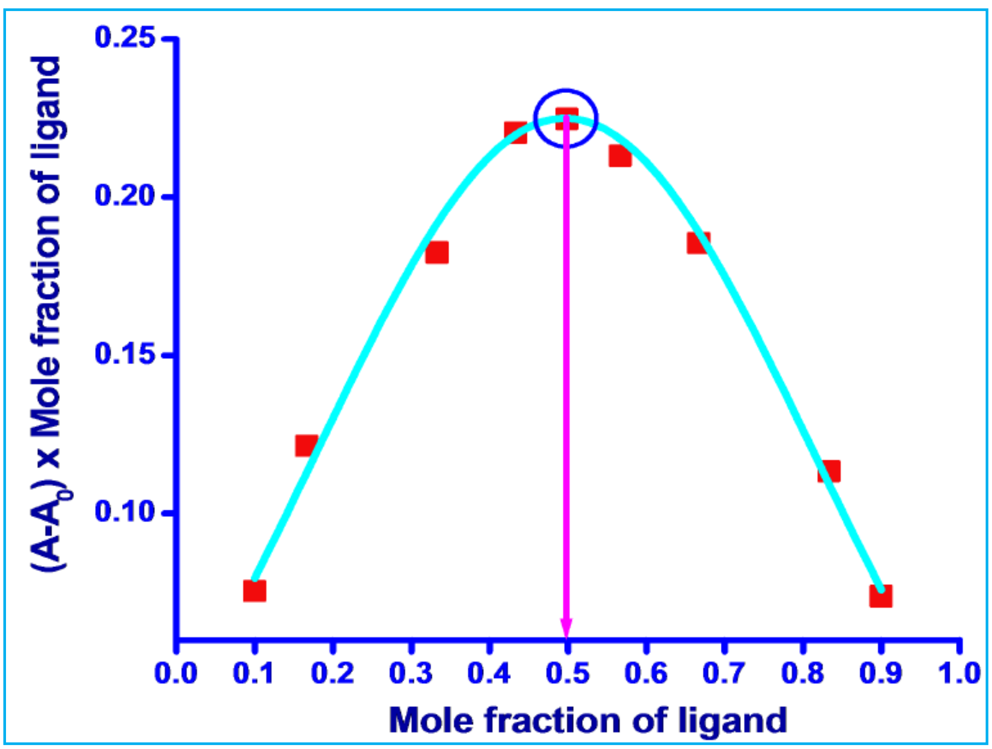

Figure S21. Job's plot for determination of stoichiometry of Al^{3+}: **4h** complex in solution.

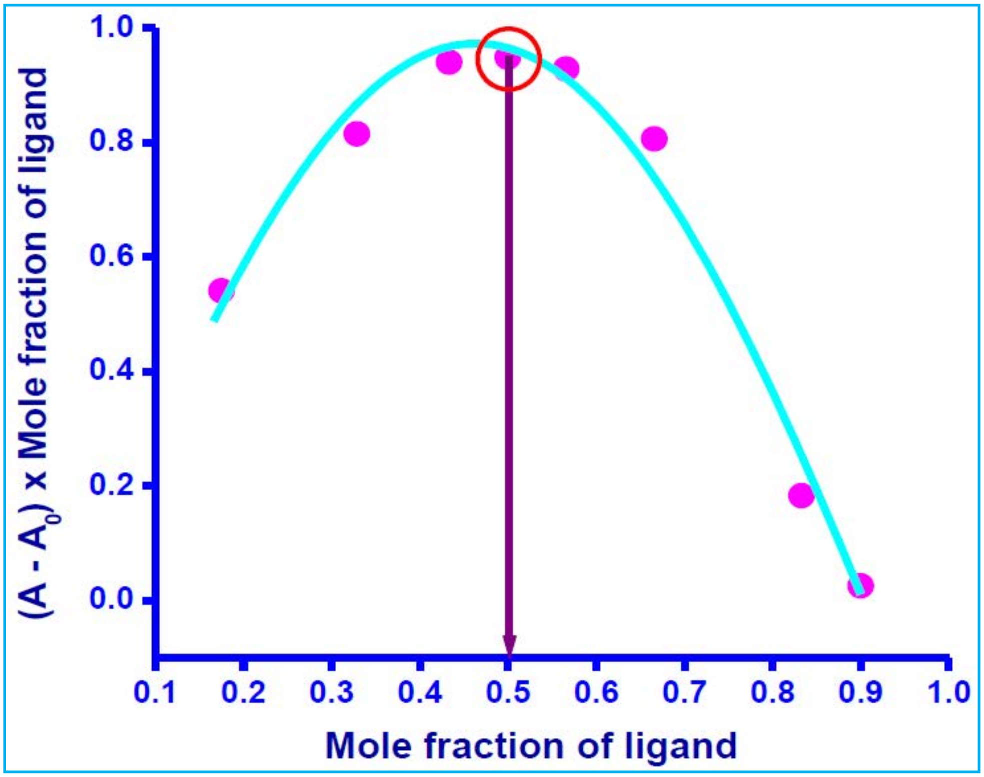

Figure S22. Job′s plot for determination of stoichiometry of Al^{3+} : **6g** complex in solution.

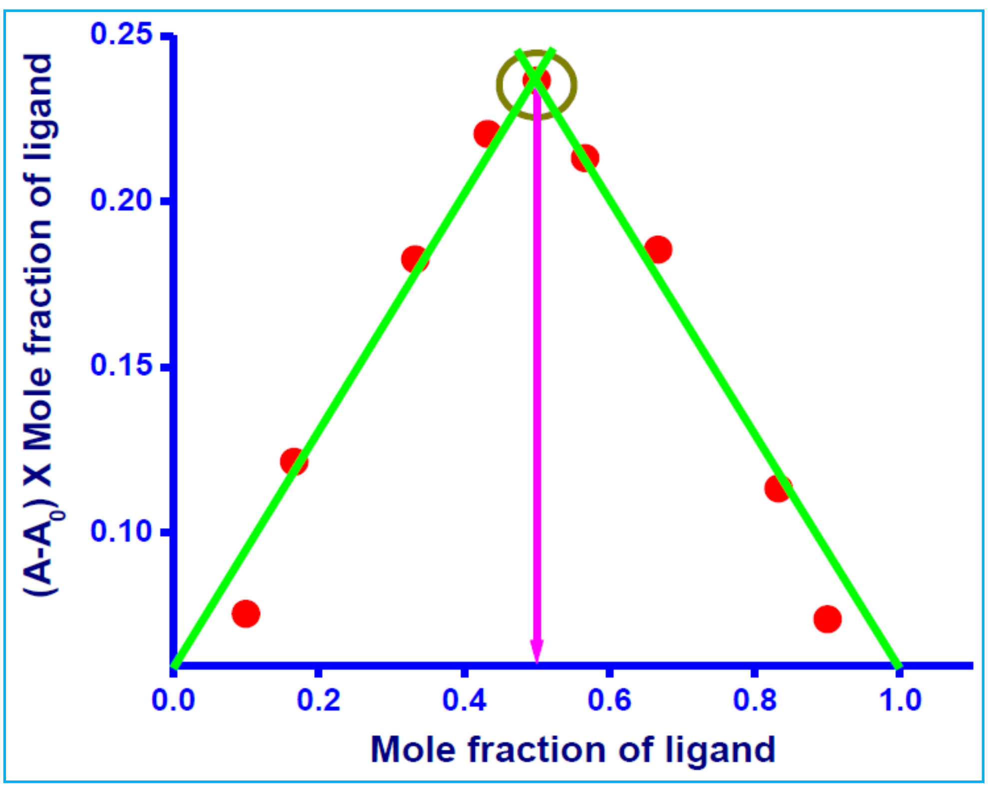

Figure S23. Job′s plot for determination of stoichiometry of Al^{3+} : **6j** complex in solution.

According to the linear Benesi–Hildebrand expression, the measured fluorescence intensity $(F - F_0)/(F_x - F_0)$ varied as a function of $1/[Al^{3+}]$ in a linear relationship, which indicates the formation of 1 : 1 stoichiometry between Al^{3+} and chemosensors (4a, 4e, 4g, 4h, 6g, 6j) in the complex.

$$\frac{1}{F_X - F_0} = \frac{1}{F_{max} - F_0} + \frac{1}{K[C]}\left(\frac{1}{F_{max} - F_0}\right)$$

where F_0, F_x and F_{max} are the emission intensities of organic moiety considered in the absence of Al^{3+} ions, at an intermediate Al^{3+} concentration and at a concentration of complete interaction, respectively, K is the binding constant and $[C]$ is the concentration of Al^{3+} ions.

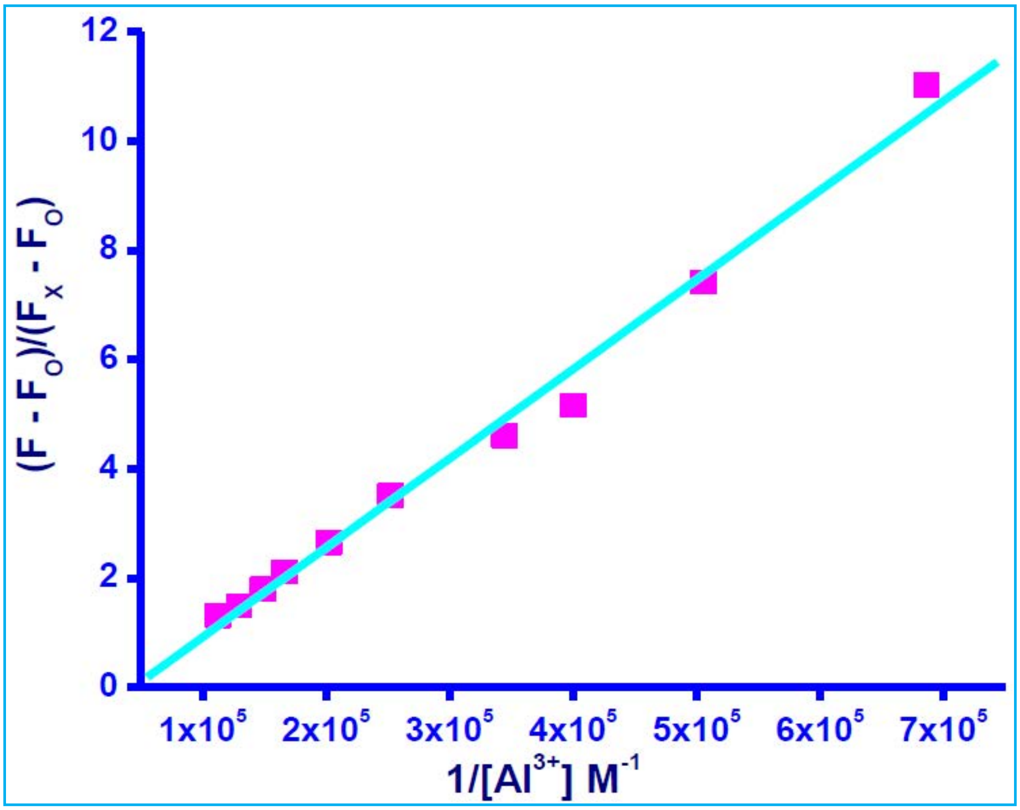

Figure S24. Benesi-Hildebrand plot $[(F\text{-}F_0)/(F_x\text{-}F_0)]$ vs. $1/[Al^{3+}]$ for complexation between **4a** and Al^{3+} derived from emission titration curve.

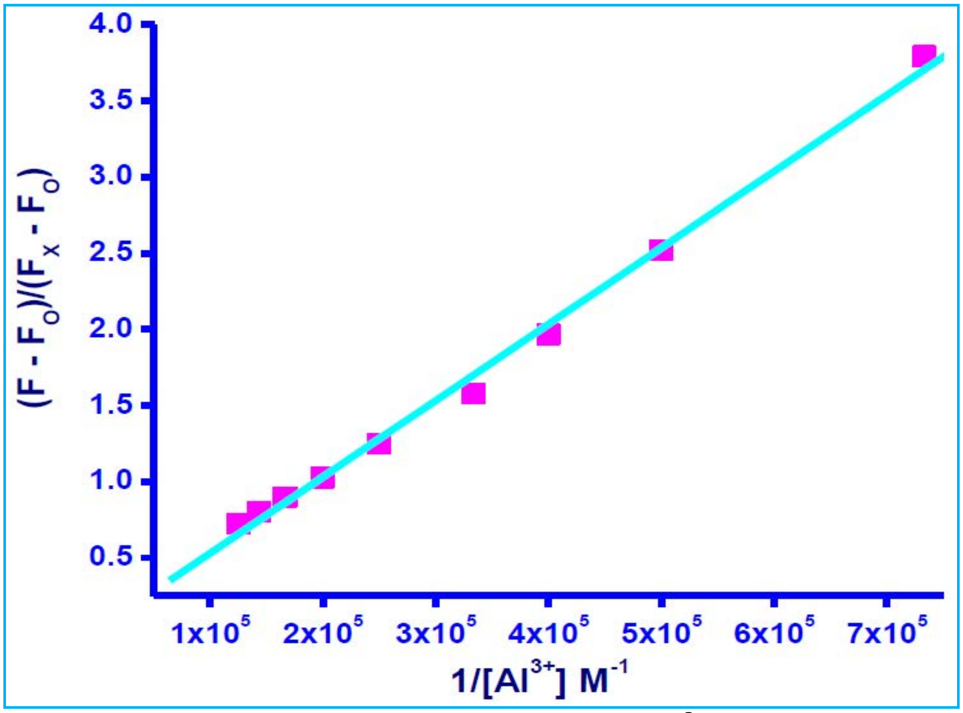

Figure S25. Benesi-Hildebrand plot [(F-F_0)/(F_x-F_0)] vs. 1/ [Al^{3+}] for complexation between **4e** and Al^{3+} derived from emission titration curve.

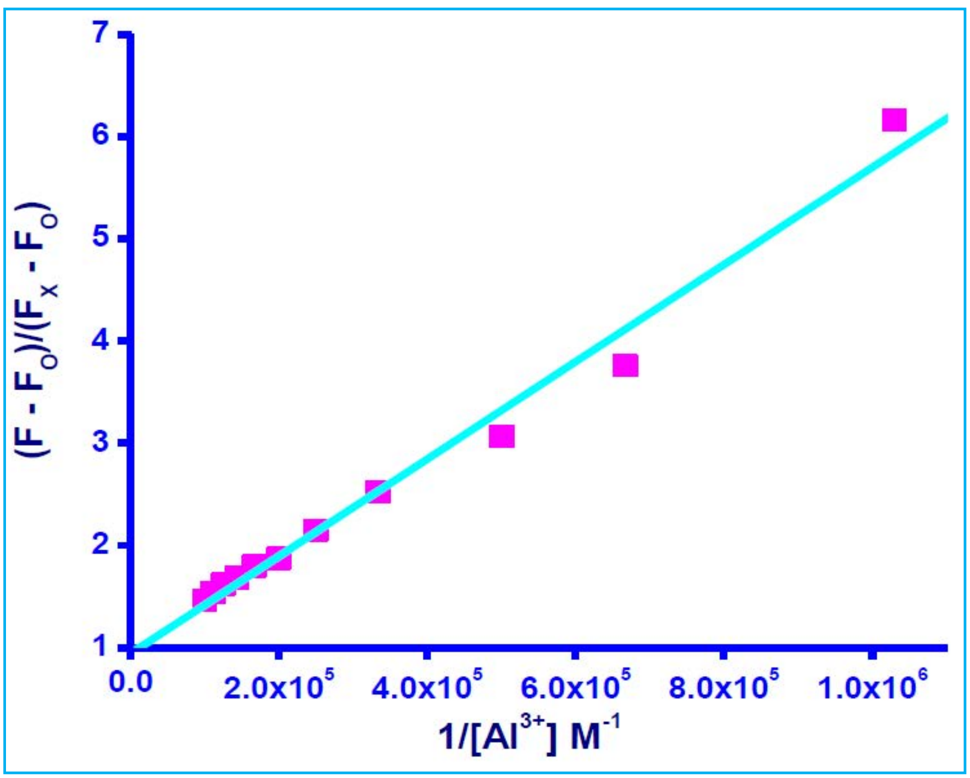

Figure S26. Benesi-Hildebrand plot [(F-F_0)/(F_x-F_0)] vs. 1/ [Al^{3+}] for complexation between **4g** and Al^{3+} derived from emission titration curve.

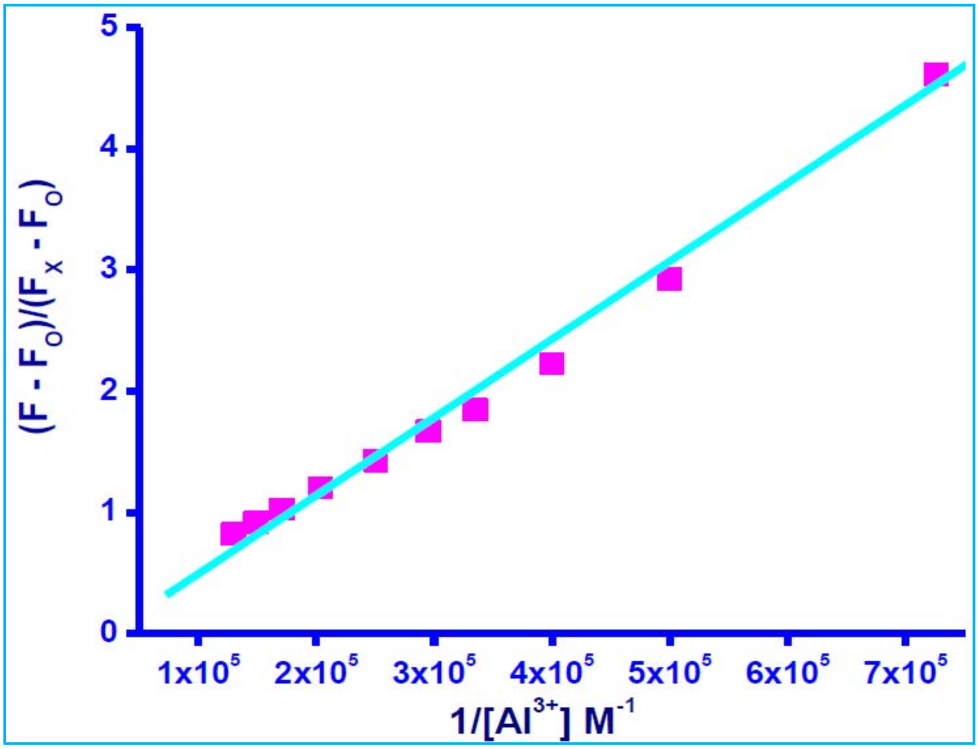

Figure S27. Benesi-Hildebrand plot [(F-F$_0$)/(F$_x$-F$_0$)] vs. 1/ [Al^{3+}] for complexation between **4h** and Al^{3+} derived from emission titration curve.

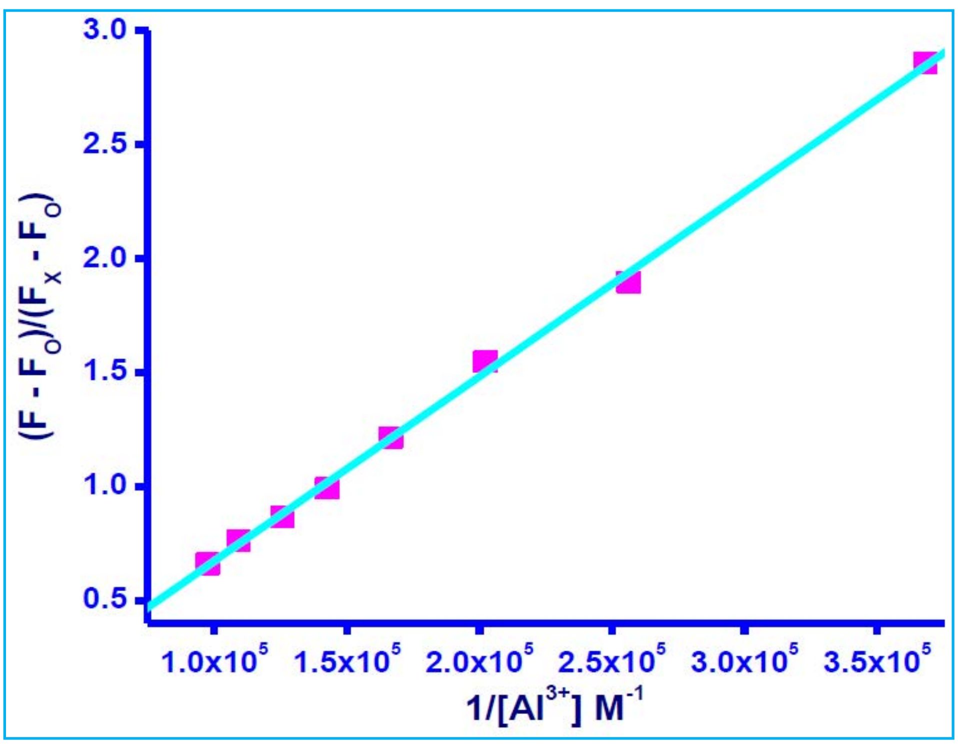

Figure S28. Benesi-Hildebrand plot [(F-F$_0$)/(F$_x$-F$_0$)] vs. 1/ [Al^{3+}] for complexation between **6g** and Al^{3+} derived from emission titration curve.

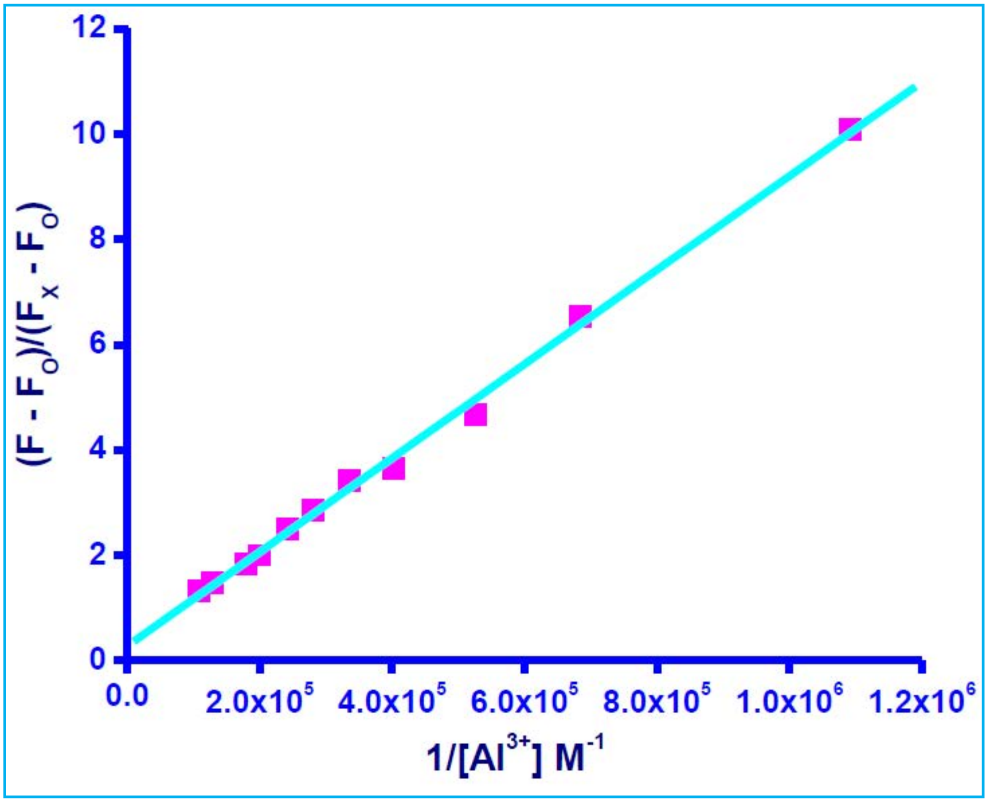

Figure S29. Benesi-Hildebrand plot [(F-F$_0$)/(F$_x$-F$_0$)] vs. 1/ [Al^{3+}] for complexation between **6j** and Al^{3+} derived from emission titration curve.

<u>**Detection limit** calculation in emission spectroscopy</u>

The limit of detection (LOD) of compounds (**4a, 4e, 4h, 4g, 6j, 6g**) with Al^{3+} was measured on the basis of fluorescence titration measurement. The detection limit was calculated using the following equation:

$$\boldsymbol{DL = K \times \frac{\sigma}{S}}$$

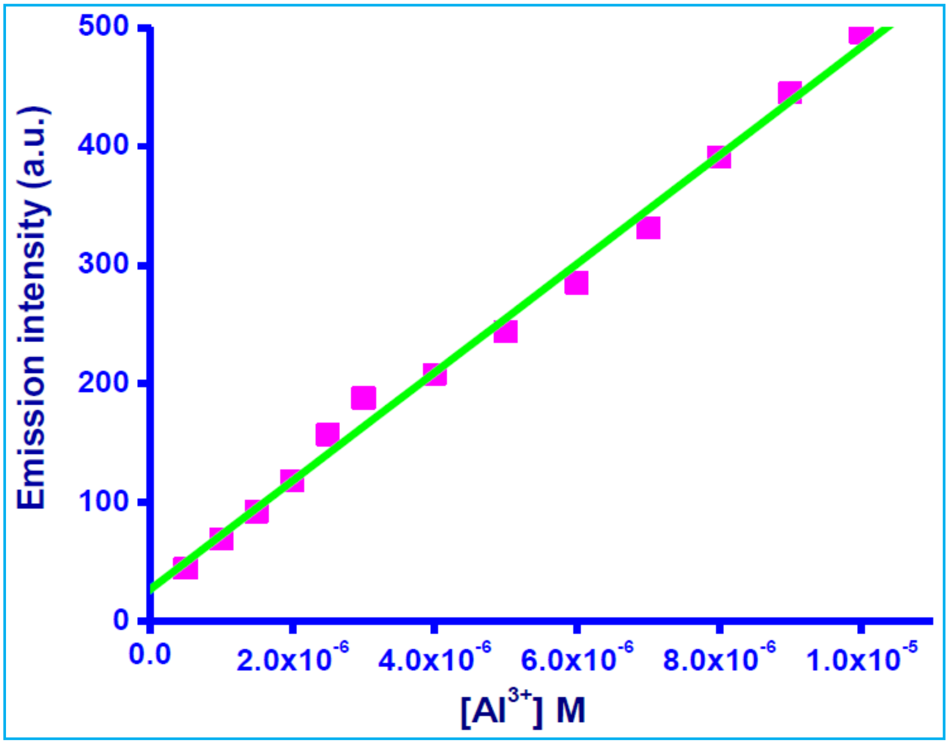

Figure S30. The limit of detection (LOD) of **4a** for Al^{3+} as a function of [Al^{3+}].

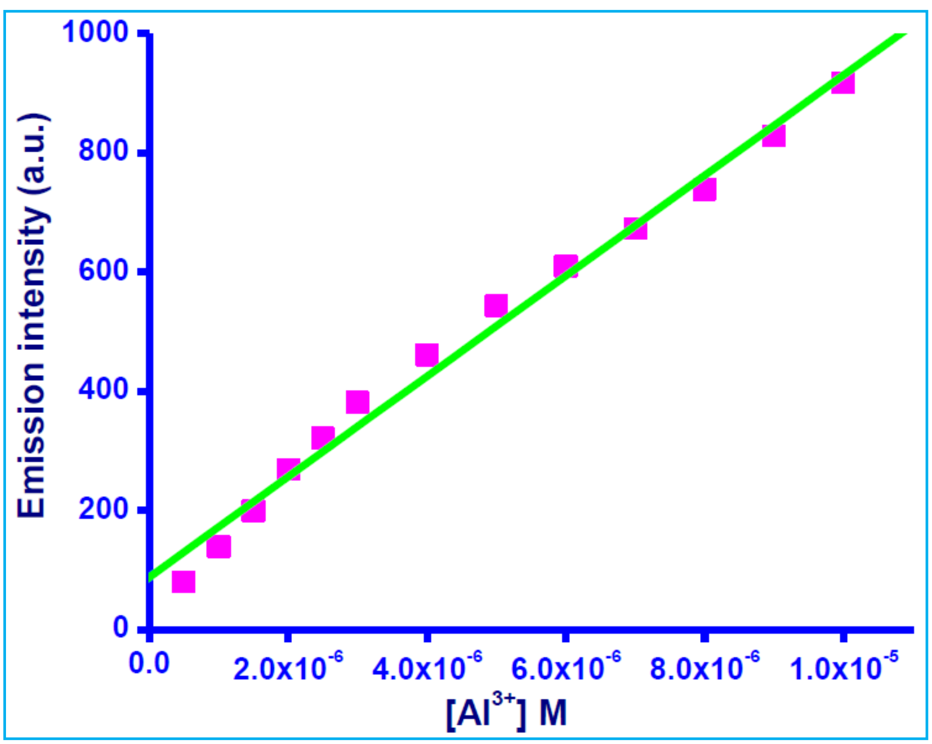

Figure S31. The limit of detection (LOD) of **4e** for Al^{3+} as a function of [Al^{3+}].

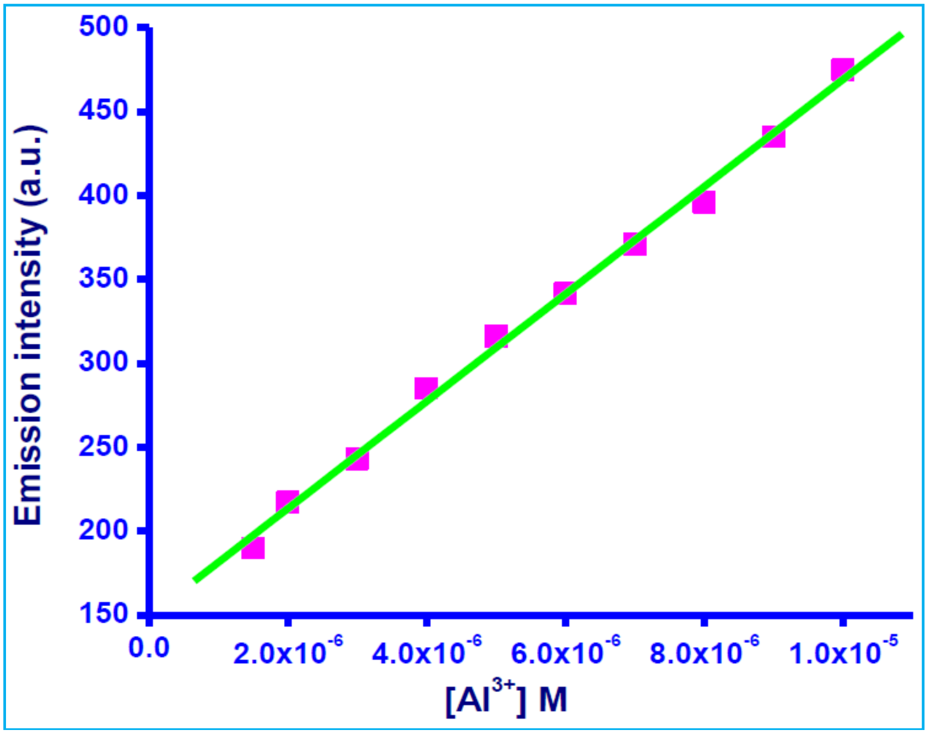

Figure S32. The limit of detection (LOD) of **4g** for Al^{3+} as a function of $[Al^{3+}]$.

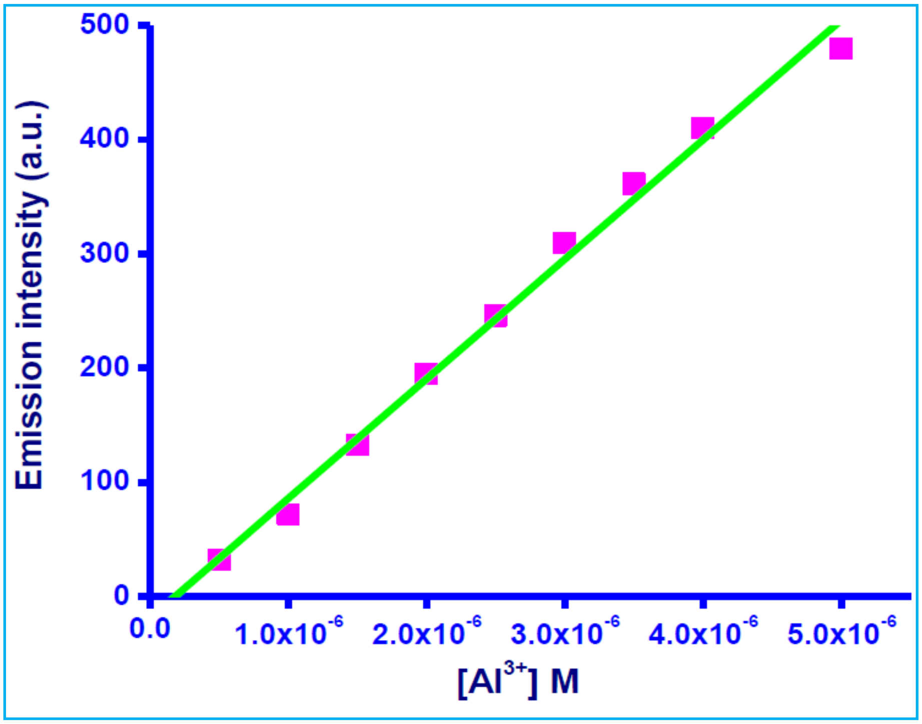

Figure S33. The limit of detection (LOD) of **4h** for Al^{3+} as a function of $[Al^{3+}]$.

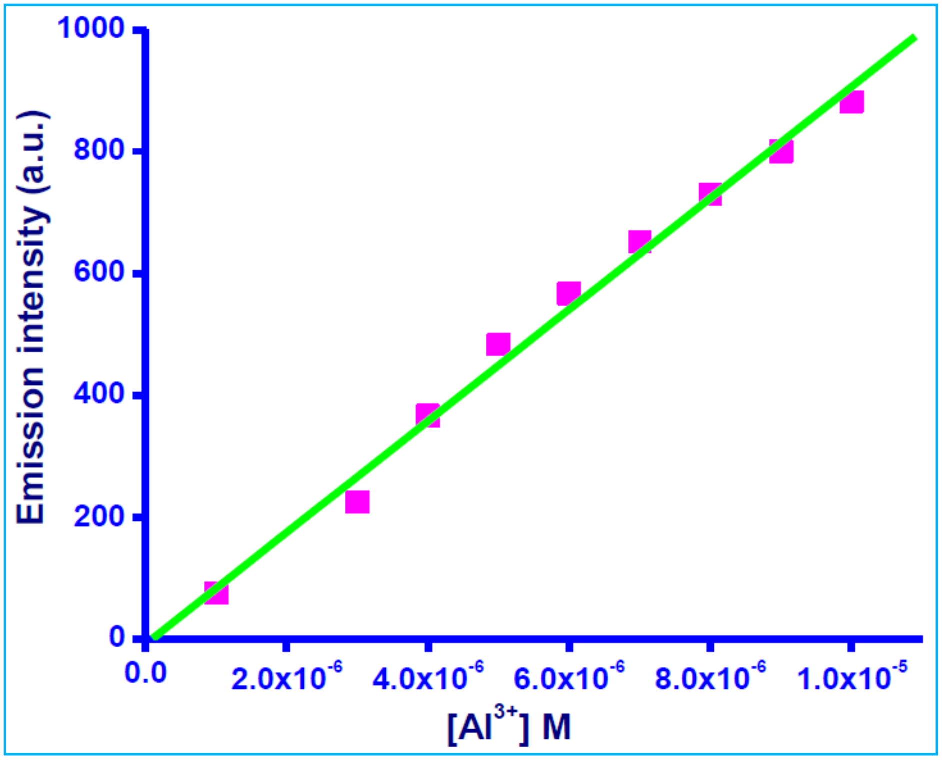

Figure S34. The limit of detection (LOD) of **6g** for Al^{3+} as a function of [Al^{3+}].

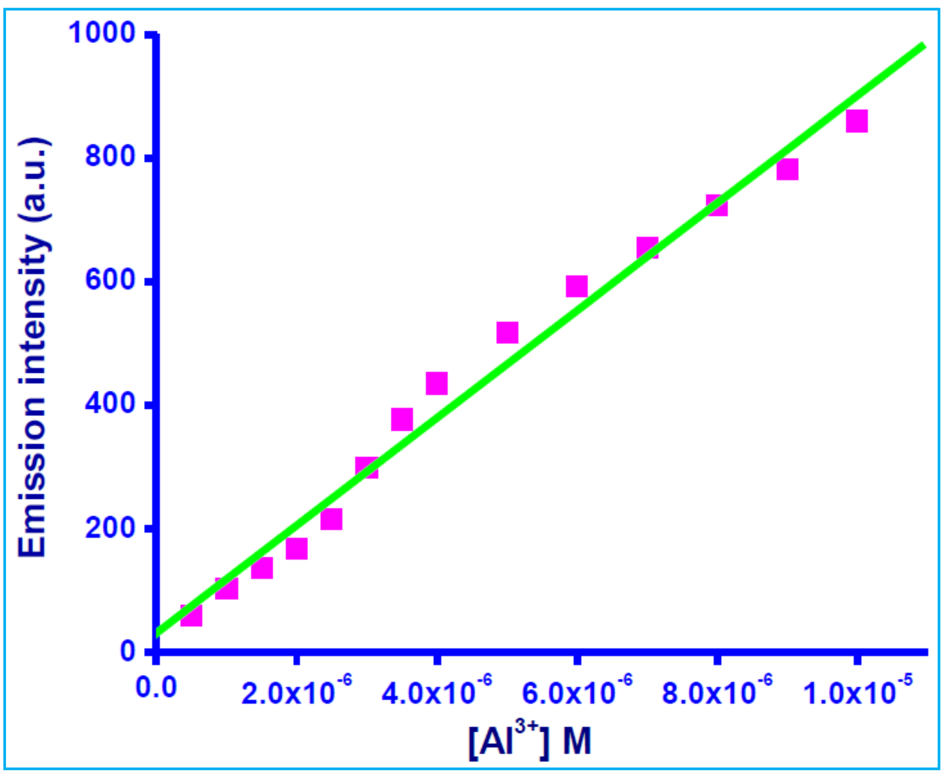

Figure S35. The limit of detection (LOD) of **6j** for Al^{3+} as a function of [Al^{3+}].

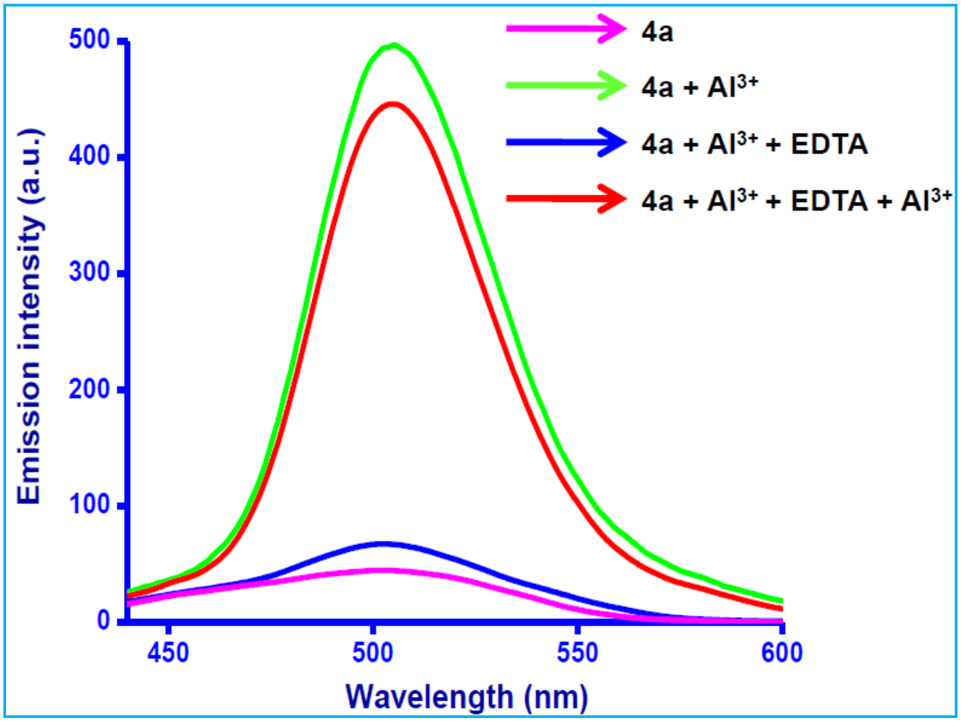

Figure S36. Fluorescence emission spectra of chemosensor (**4a**) in the presence of Al^{3+} ion followed by addition of EDTA.

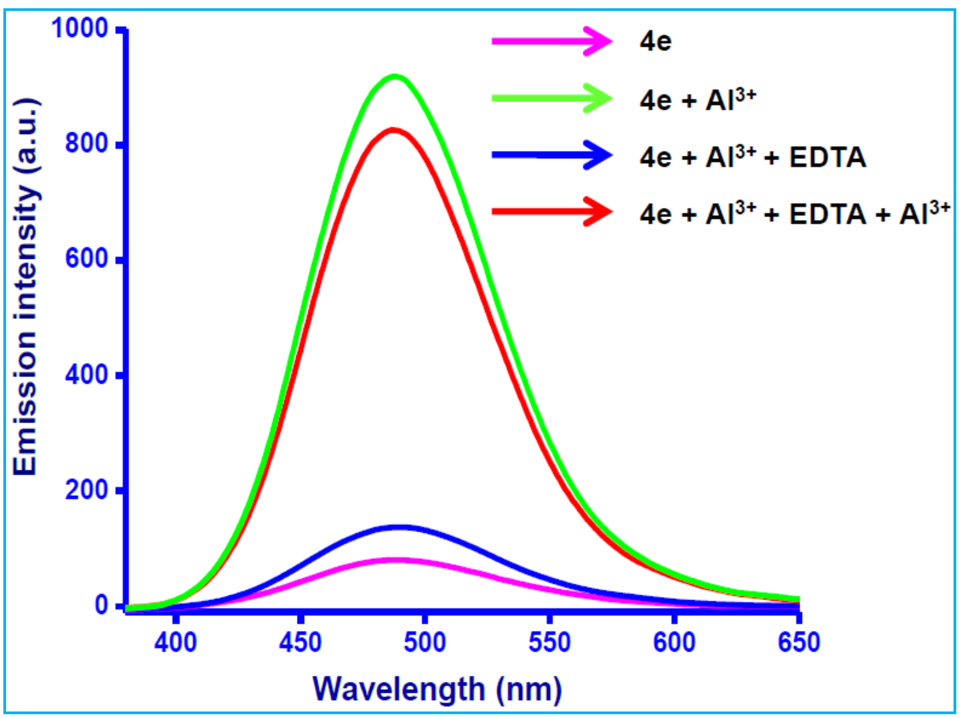

Figure S37. Fluorescence emission spectra of chemosensor (**4e**) in the presence of Al^{3+} ion followed by addition of EDTA.

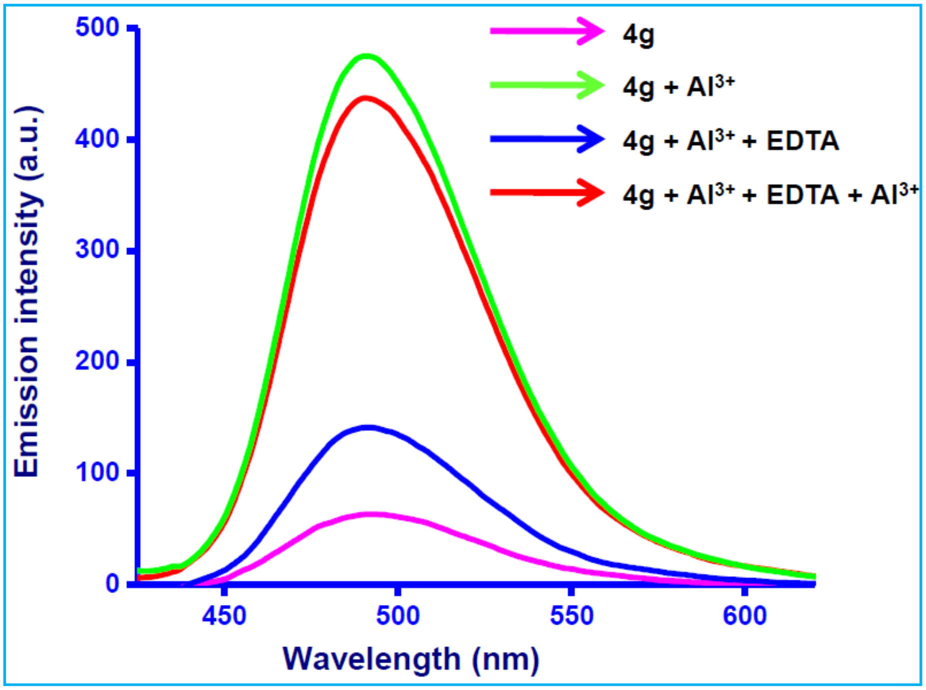

Figure S38. Fluorescence emission spectra of chemosensor (**4g**) in the presence of Al^{3+} ion followed by addition of EDTA.

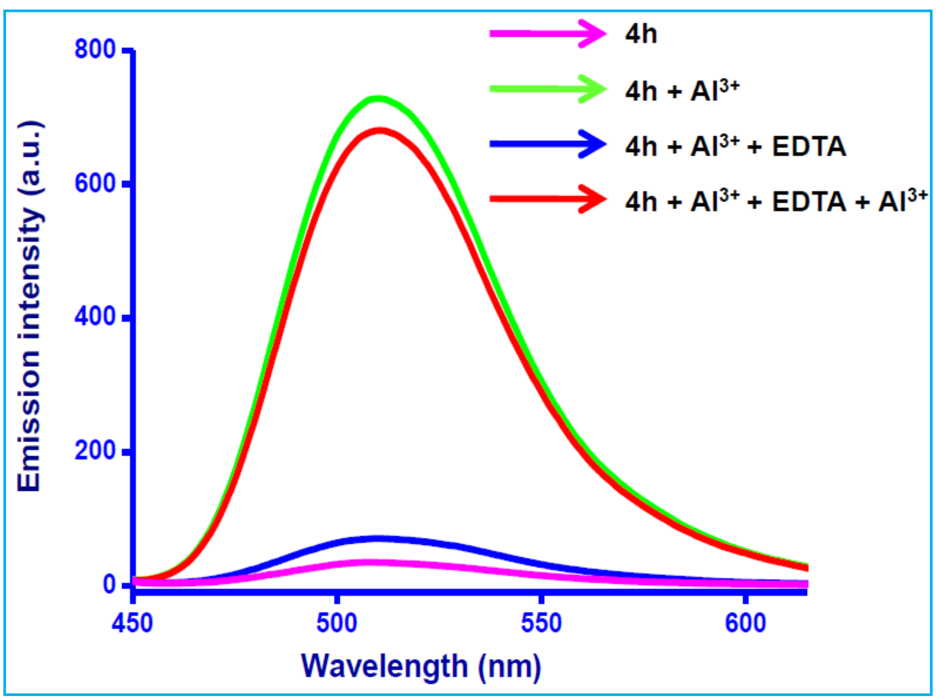

Figure S39. Fluorescence emission spectra of chemosensor (**4h**) in the presence of Al^{3+} ion followed by addition of EDTA.

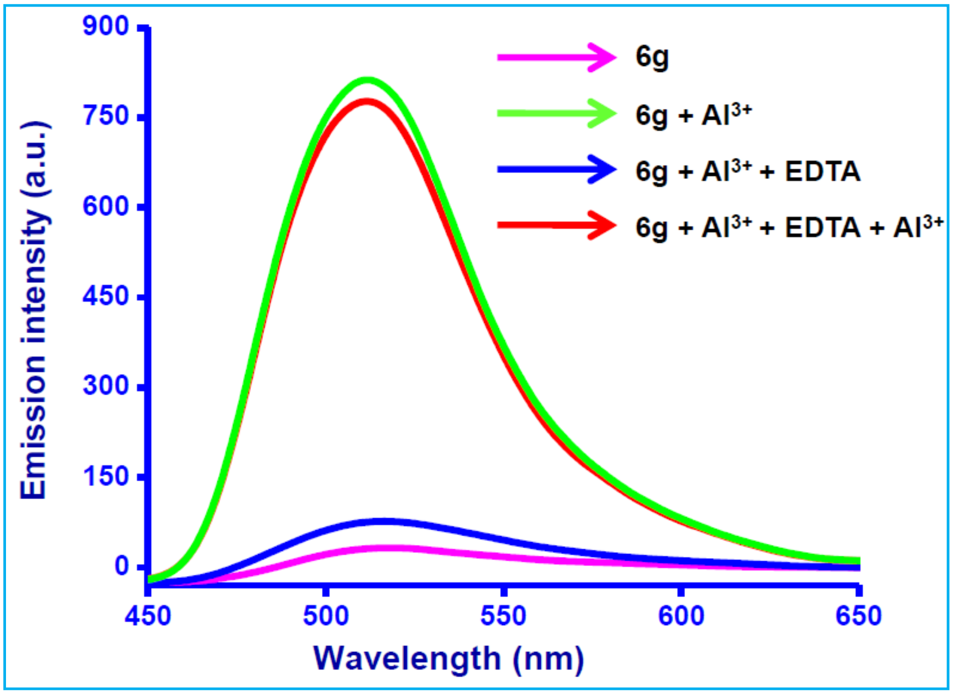

Figure S40. Fluorescence emission spectra of chemosensor (**6g**) in the presence of Al^{3+} ion followed by addition of EDTA.

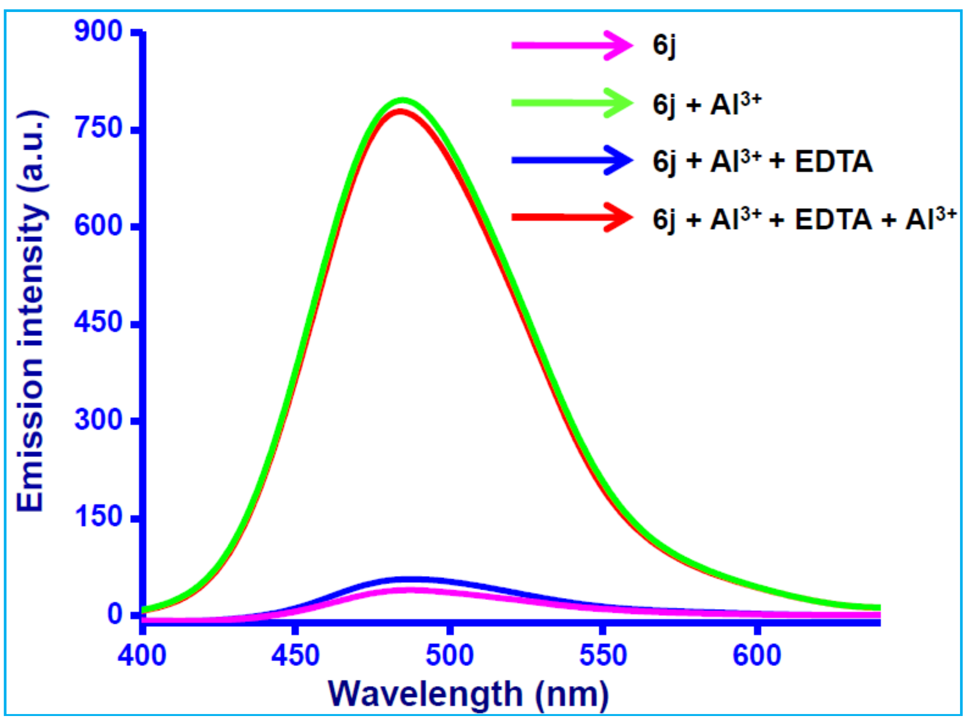

Figure S41. Fluorescence emission spectra of chemosensor (**6j**) in the presence of Al^{3+} ion followed by addition of EDTA.

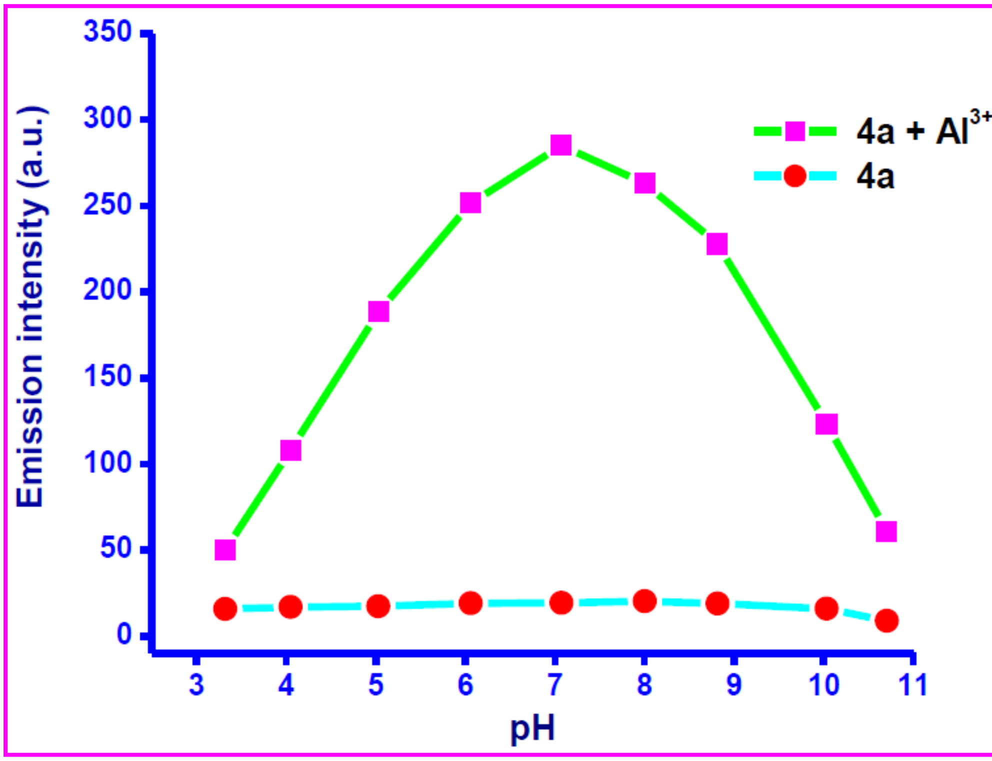
Emission intensity (a.u.)
350
300
250
200
150
100
50
0
3
4
5
6
7
8
9
10
11
pH
4a + Al3+
4a
4a

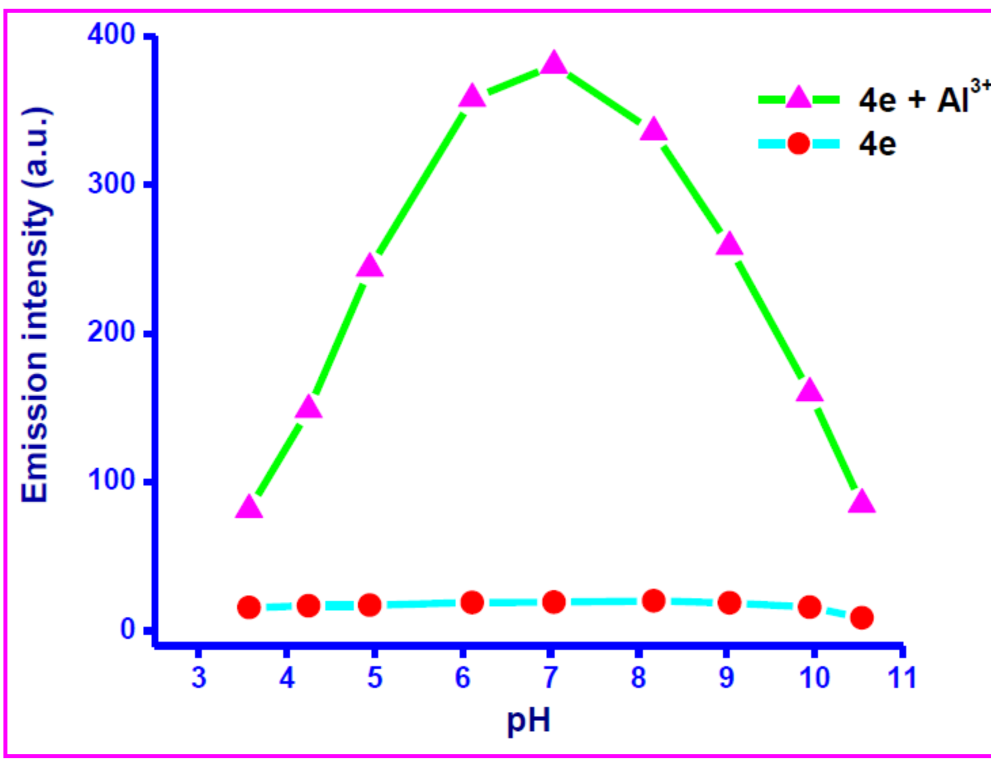
Emission intensity (a.u.)
400
300
200
100
0
3
4
5
6
7
8
9
10
11
pH
4e + Al3+
4e
4e

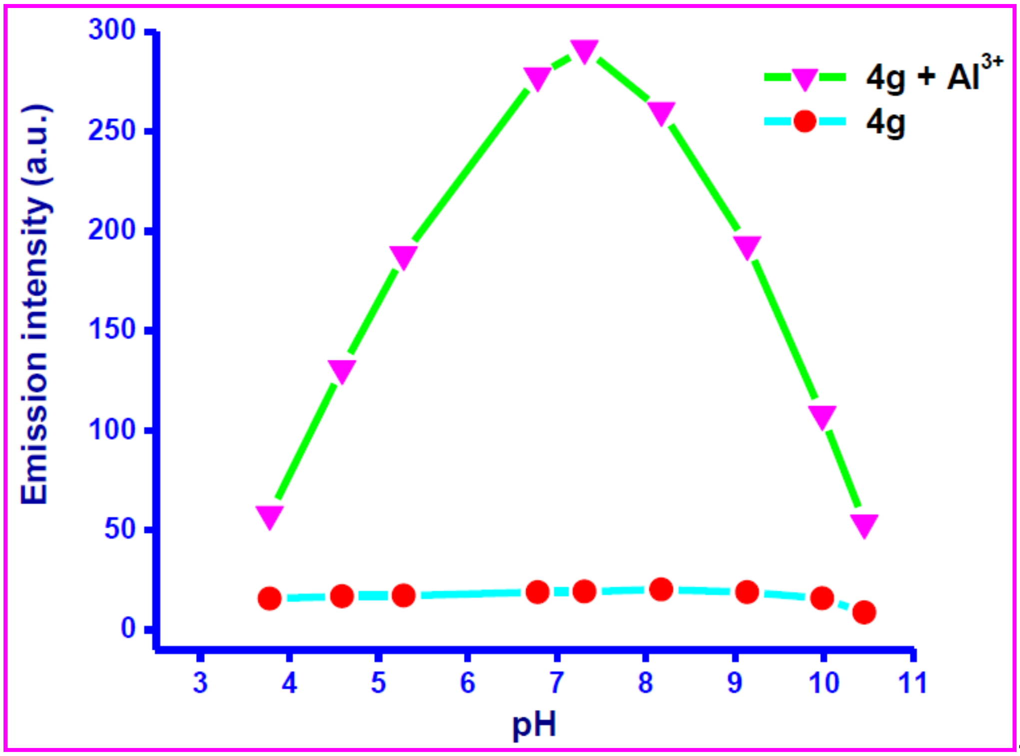

Emission intensity (a.u.)
300
250
200
150
100
50
0
3
4
5
6
7
8
9
10
11
pH
4g + Al3+
4g

4g

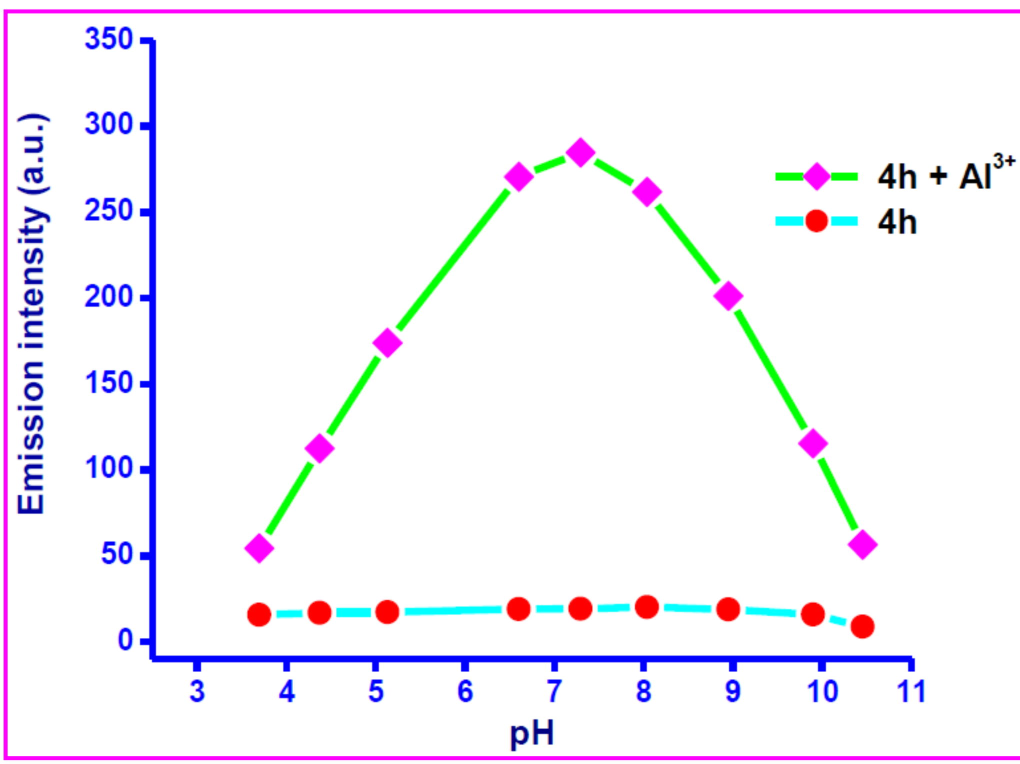

Emission intensity (a.u.)
350
300
250
200
150
100
50
0
3
4
5
6
7
8
9
10
11
pH
4h + Al3+
4h

4h

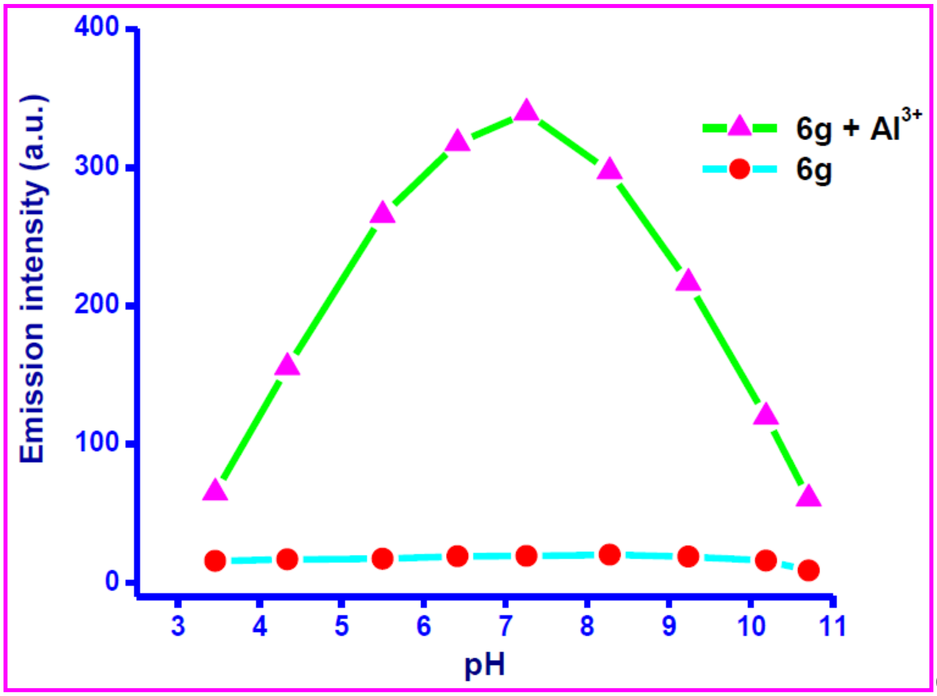

6g

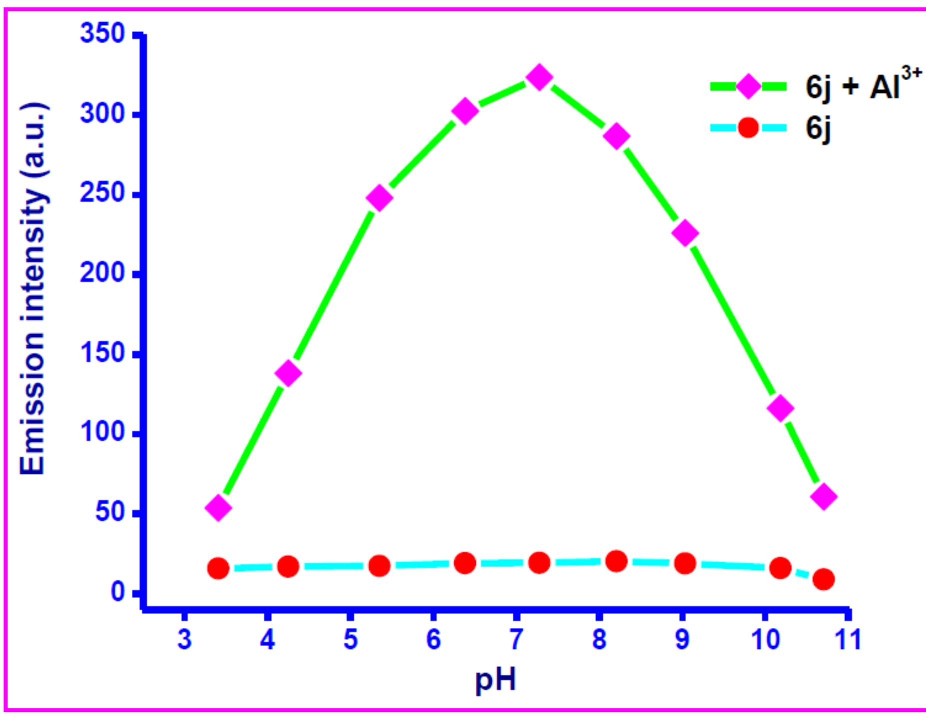

6j

Figure S42. Emission intensity of compounds **4a, 4e, 4g, 4h, 6g and 6j** in absence and in presence of Al^{3+} at different pH values in aqueous DMSO solution.

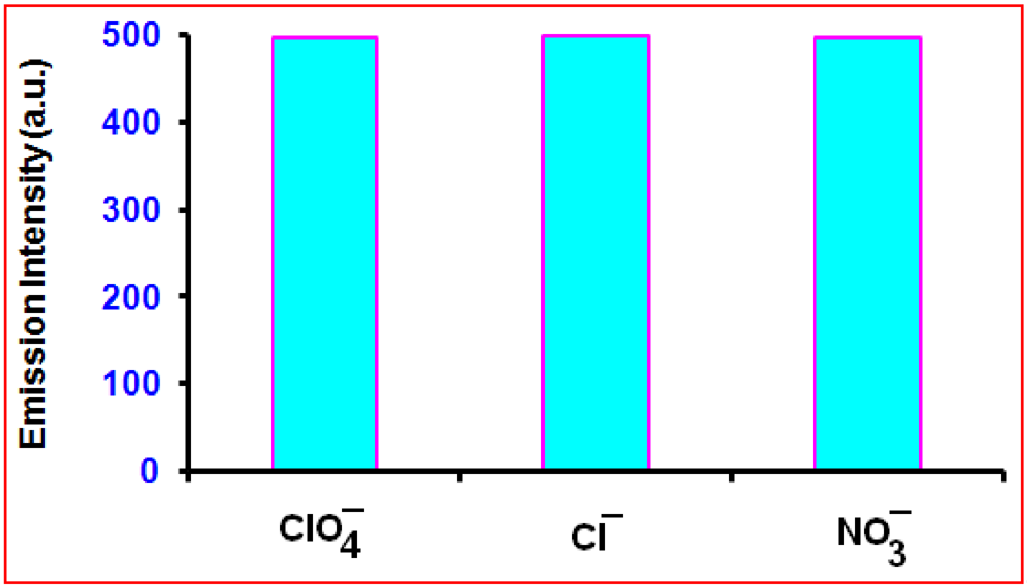

4a

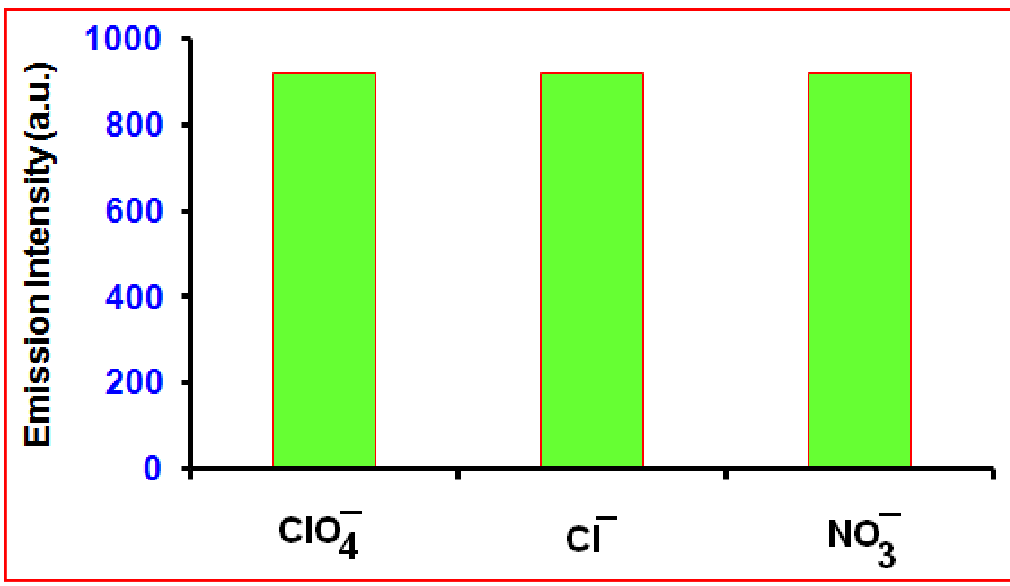

4e

Figure 43. Anion independency of emission intensity of **4a** and **4e** in presence of various Al^{3+} salts [e.g. $Al(ClO_4)_3$, $AlCl_3$ and $Al(NO_3)_3$].

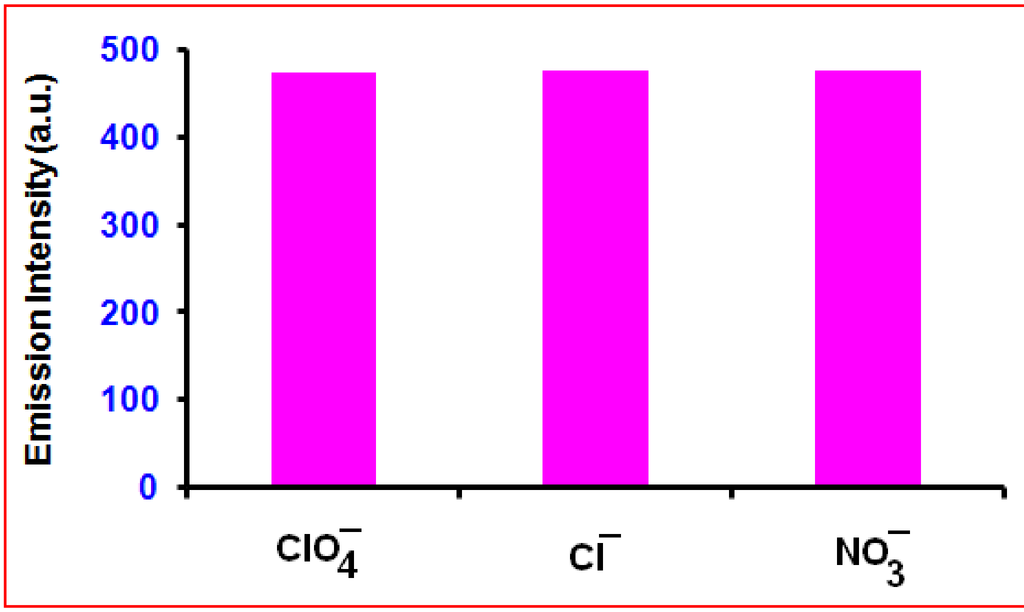

4g

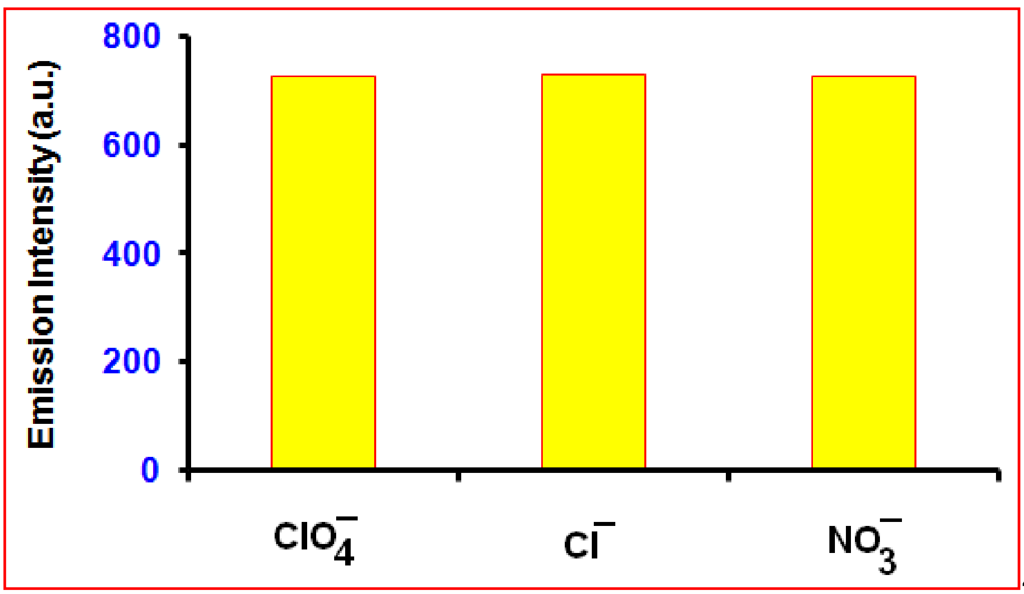

4h

Figure 44. Anion independency of emission intensity of **4g** amd **4h** in presence of various Al^{3+} salts [e.g. $Al(ClO_4)_3$, $AlCl_3$ and $Al(NO_3)_3$].

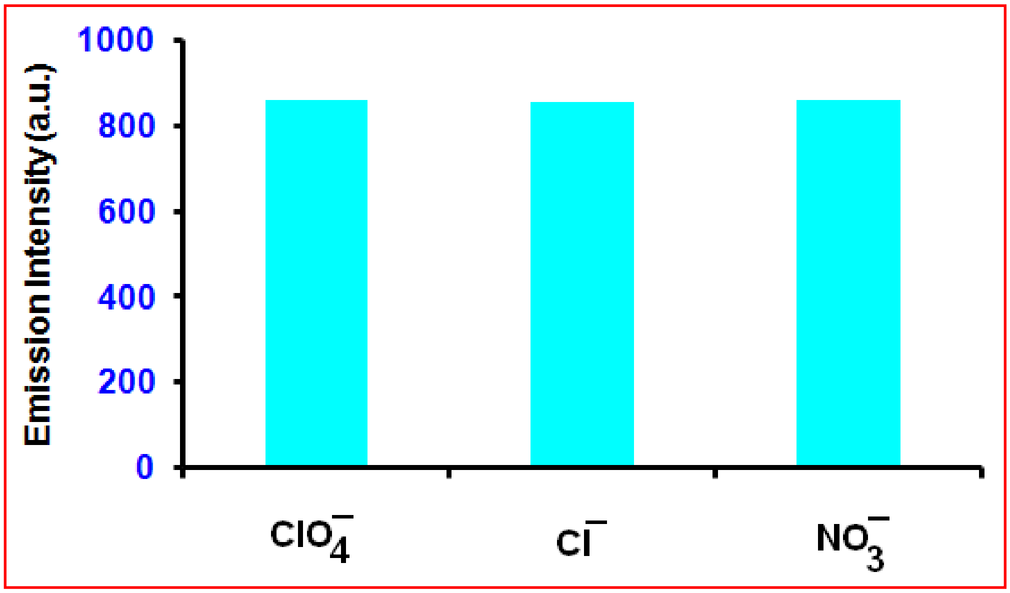

Figure 45. Anion independency of emission intensity of **6j** in presence of various Al^{3+} salts [e.g. $Al(ClO_4)_3$, $AlCl_3$ and $Al(NO_3)_3$].

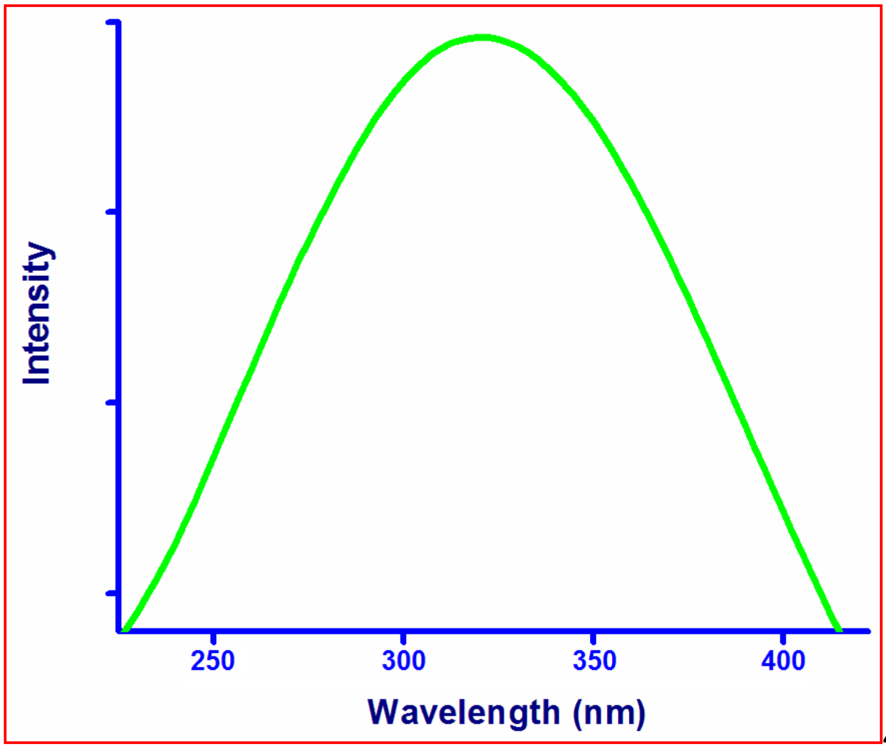

4a

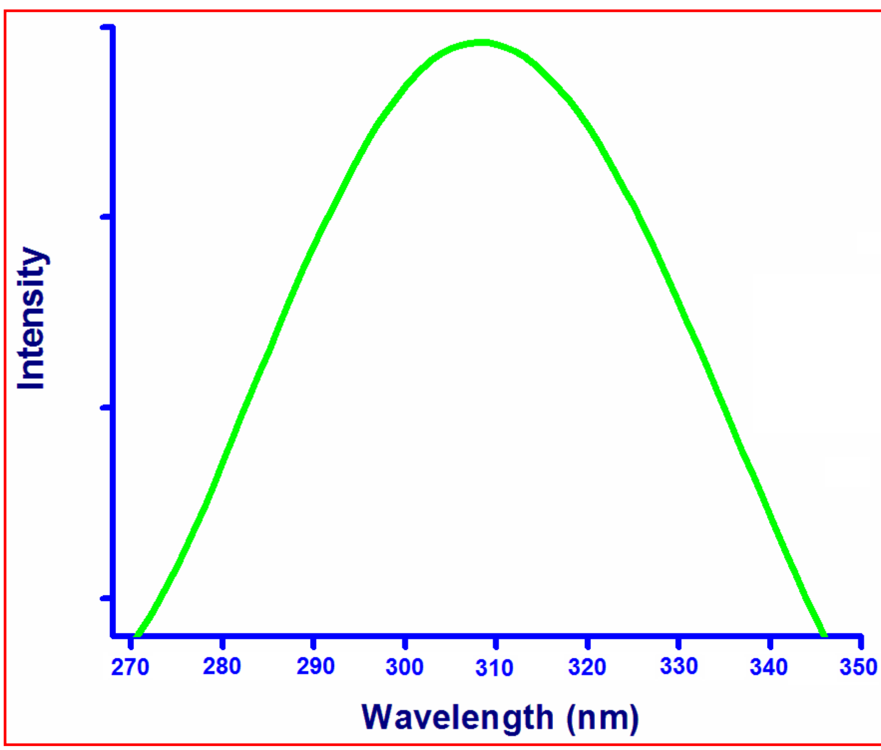

4e

Figure 46. Excitation spectra of **4a** and **4e** in presence of Al^{3+} in solution.

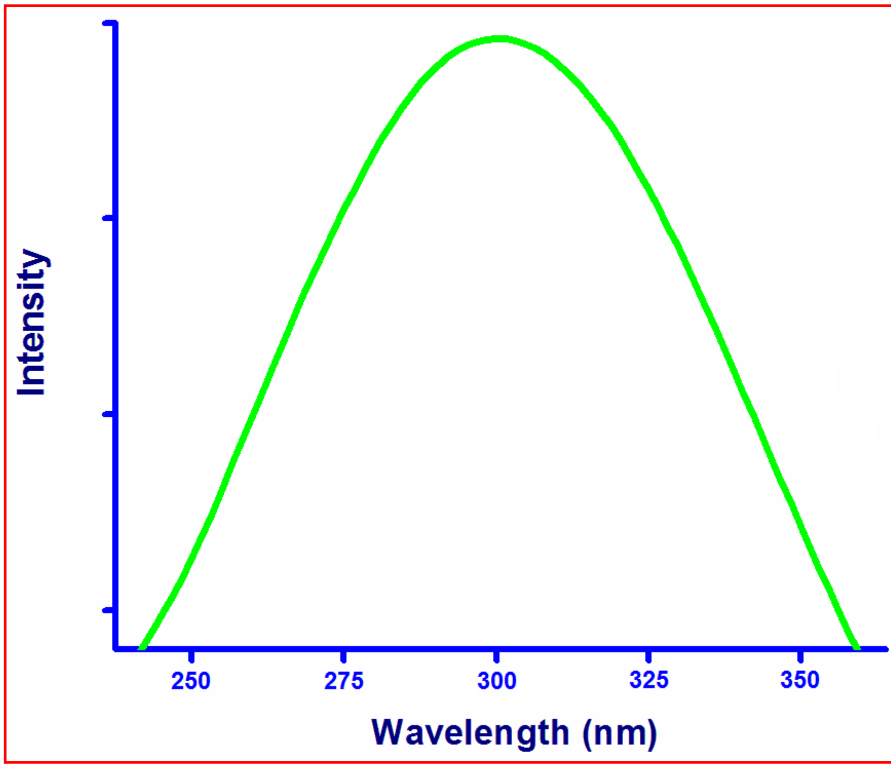

4g

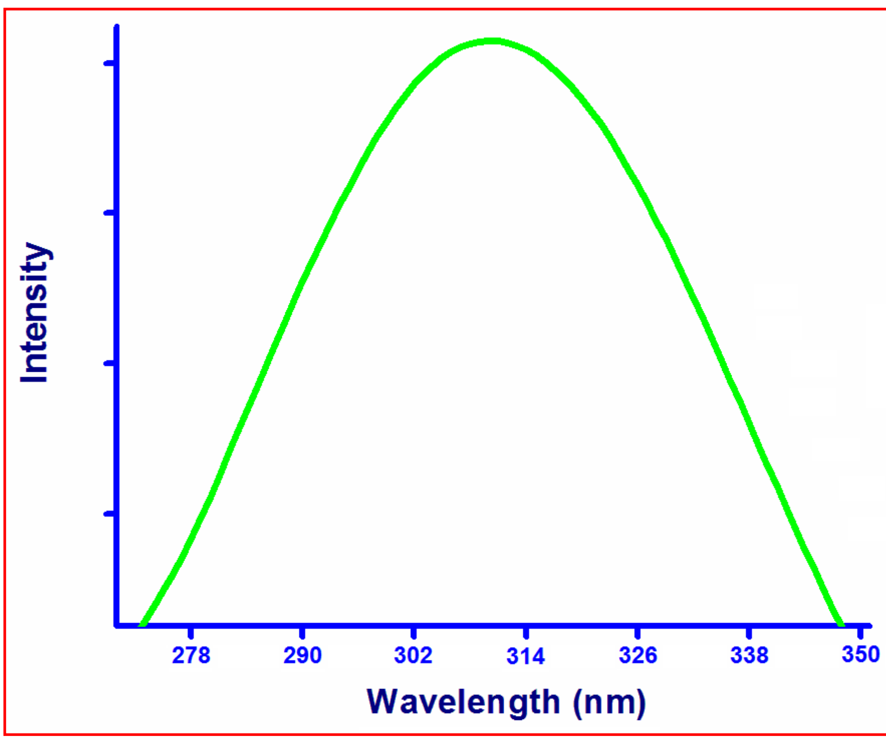

4h

Figure 47. Excitation spectra of **4g** and **4h** in presence of Al^{3+} in solution.

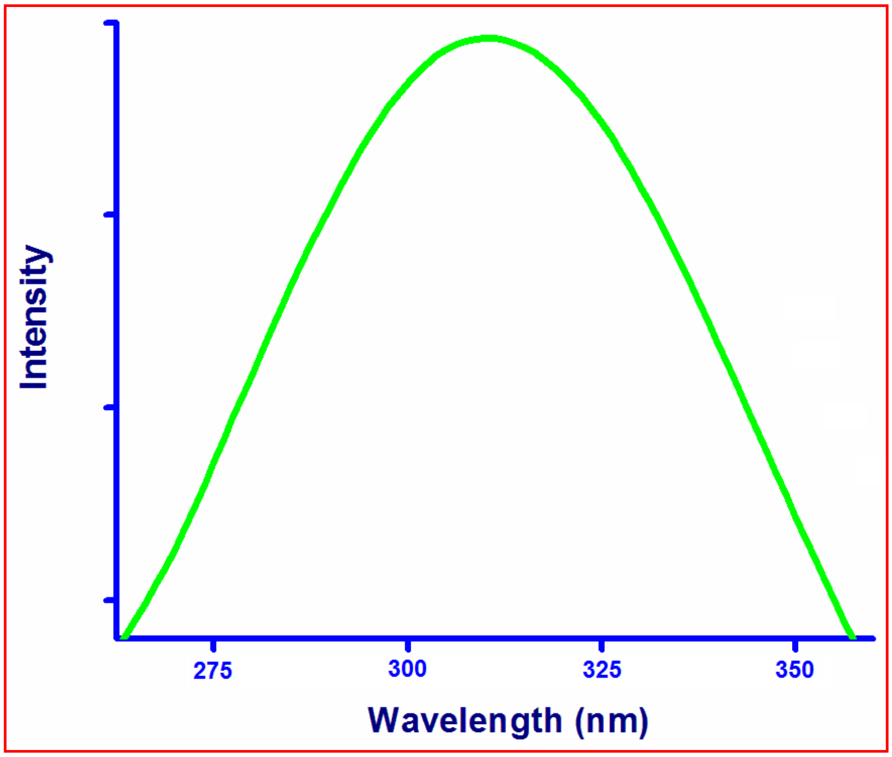

6g

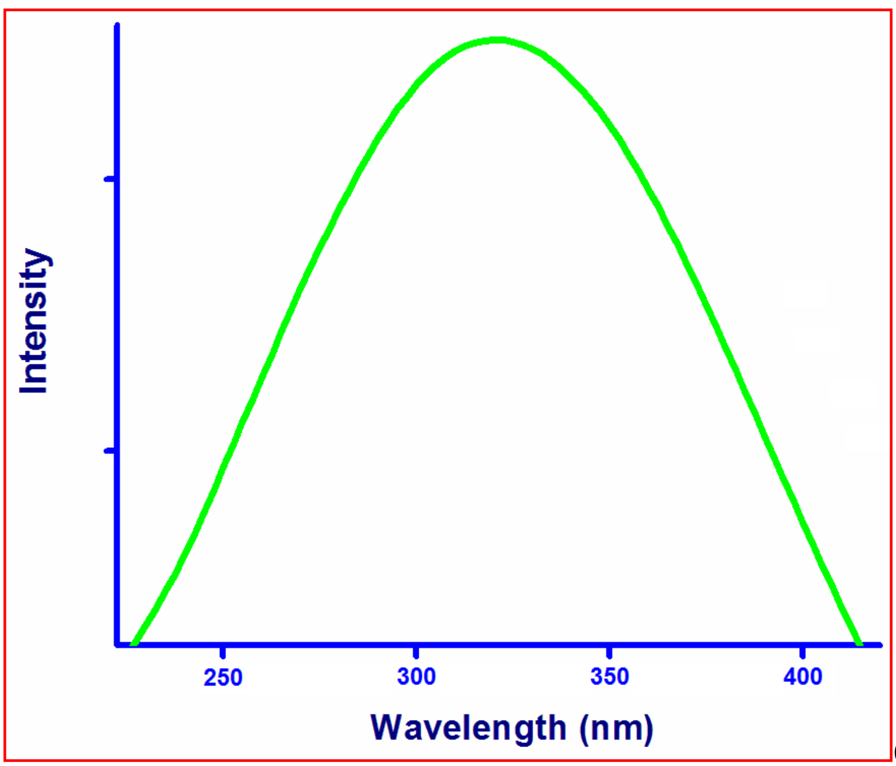

6j

Figure 48. Excitation spectra of **6j** in presence of Al^{3+} in solution.

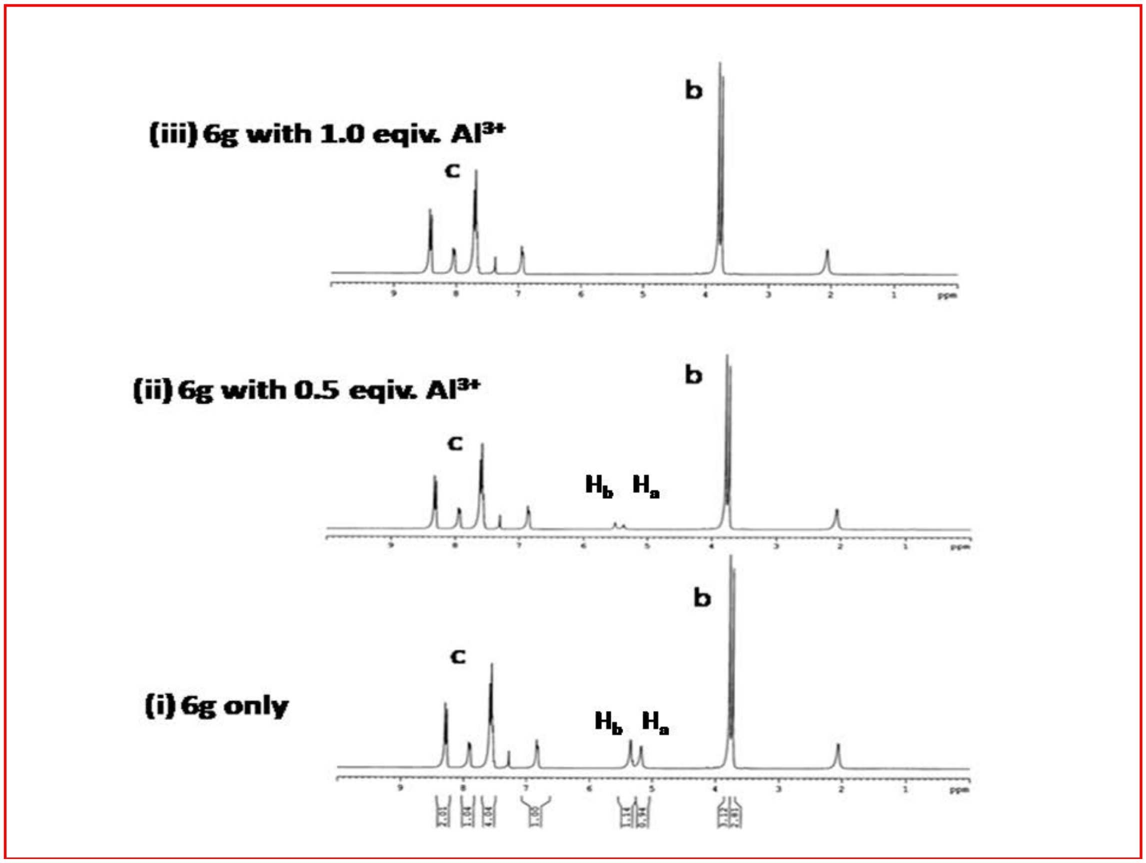

Figure 49. **^{1}H** NMR titration of chemosensor **6j** with Al^{3+} ion in DMSO- d_6 solvent.

Table S4. Summary of photophysical properties of compounds **4a, 4e, 4g, 4h, 6g and 6j** studied in various solvents.

Compound	λ_{ex} (nm)	λ_{em} (nm)	$\Delta\lambda[\lambda_{abs} - \lambda_{em}]$ (nm)	Quantum yield (Φ_f)
DMSO				
4a	309.87	503.74	193.87	0.063
4e	307.81	487.65	179.84	0.069
4g	305.55	489.72	184.17	0.067
4h	304.95	504.19	199.24	0.065
6g	313.98	506.69	192.71	0.061
6j	318.76	484.35	165.59	0.064
DMF				
4a	310.21	502.61	192.4	0.065
4e	309.76	489.57	179.81	0.061
4g	304.77	491.87	187.10	0.062
4h	306.38	503.28	196.90	0.068
6g	310.93	508.73	197.80	0.067
6j	311.01	497.44	186.43	0.063
ACN				
4a	311.81	505.52	193.71	0.067
4e	306.54	492.38	185.84	0.064
4g	305.32	493.74	188.42	0.069
4h	307.43	504.79	197.36	0.063
6g	312.13	502.43	190.30	0.071
6j	309.17	499.61	190.44	0.062
MeOH				

4a	314.82	503.14	188.32	0.063
4e	308.51	499.82	191.31	0.062
4g	313.43	493.71	180.28	0.068
4h	310.35	504.45	194.10	0.064
6g	310.18	504.63	194.45	0.067
6j	311.52	510.12	198.60	0.065
EtOH				
4a	313.75	504.25	190.50	0.060
4e	310.11	502.31	192.20	0.061
4g	315.62	497.68	182.06	0.067
4h	309.74	500.53	190.79	0.063
6g	311.68	506.52	194.84	0.066
6j	312.13	511.14	199.01	0.064
THF				
4a	313.24	506.78	193.54	0.061
4e	314.03	509.02	194.99	0.064
4g	316.12	508.59	192.47	0.065
4h	310.54	511.47	200.93	0.062
6g	311.85	510.31	198.46	0.070
6j	313.24	513.35	200.11	0.068
DCM				
4a	311.82	510.02	198.20	0.060
4e	316.14	512.86	196.72	0.063
4g	313.51	513.29	199.78	0.067
4h	307.38	503.64	196.26	0.065

6g	312.35	511.63	199.28	0.069
6j	315.23	514.47	199.24	0.062
$CHCl_3$				
4a	312.31	511.88	199.57	0.065
4e	316.61	513.14	196.53	0.068
4g	314.36	509.98	195.62	0.061
4h	313.28	514.59	201.31	0.063
6g	311.47	510.75	199.28	0.067
6j	310.99	512.24	201.25	0.064

Table S5. Stability constant (*K*) and Limit of detection were studied with complexation properties of the compounds (**4a, 4e, 4g, 4h, 6g and 6j).**

Compound	Quantum yield (Φ_f)	Stability constant (*K*) (M^{-1})	Limit of detection (LOD) (M)
4a	0.064 (Free **4a**) 0.265 (**4a** + Al^{3+})	30.42×10^4	6.69×10^{-7}
4e	0.067 (Free **4e**) 0.268 (**4e** + Al^{3+})	33.85×10^4	7.52×10^{-7}
4g	0.066 (Free **4g**) 0.273 (**4g** + Al^{3+})	32.27×10^4	4.09×10^{-7}
4h	0.061 (Free **4h**) 0.276 (**4h** + Al^{3+})	37.60×10^4	8.41×10^{-7}
6g	0.063 (Free **6g**) 0.281 (**6g** + Al^{3+})	38.46×10^4	6.37×10^{-7}
6j	0.068 (Free **6j**) 0.279 (**6j** + Al^{3+})	36.33×10^4	7.84×10^{-7}

Table S6. Comparison with recently reported probes for selective detection of Al^{3+} ion.

Probes	Detection limit	Binding constant	Ref.
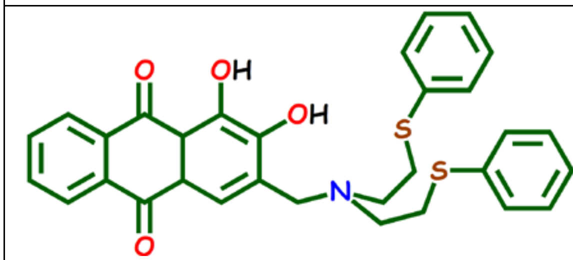	5.0×10^{-7} M	8.84×10^{3} M^{-1}	Org. Lett., 2011, 13, 5274
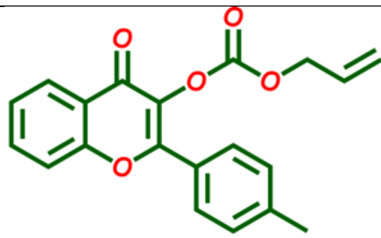	0.75 μM	4.9×10^{4} M^{-1}	Sens. Actuators B, 2018, 264, 304
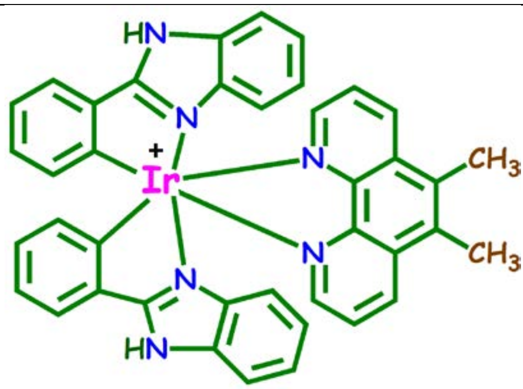	0.02 μM	–	ACS Omega 2017, 2, 9150–9155
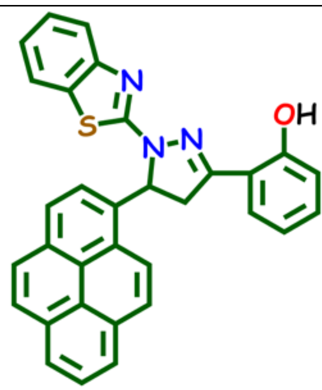	–	2.13×10^{3} M^{-1}	New J. Chem., 2018,42, 10891-10897

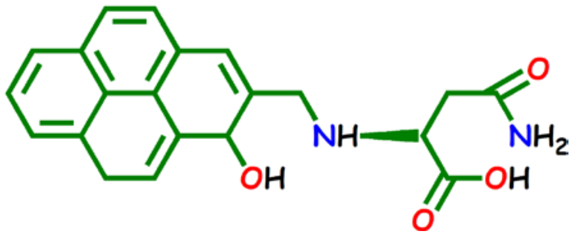	1.06 µM	1.46×10^{5} M^{-1}	Org. Lett. 2012, 14, 3420
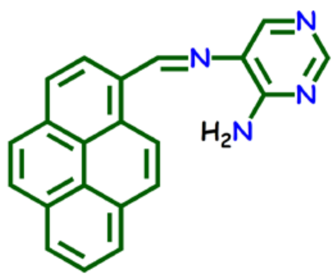	0.24×10^{-6} (M)	1240 ($M^{-1/2}$)	1. Dalton Trans., 2013,42, 4757-4763
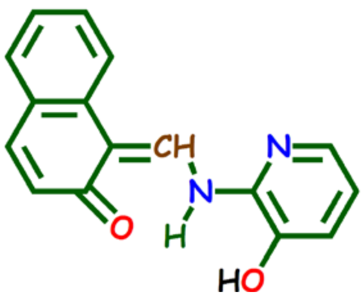	–	–	Inorg. Chem., 2013, 52, 7320
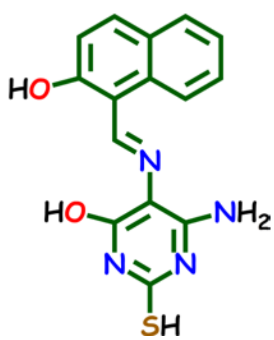	9.9×10^{-8} M	3.5×10^{4} M^{-1}	Materials Science & Engineering C 90 (2018) 468–475
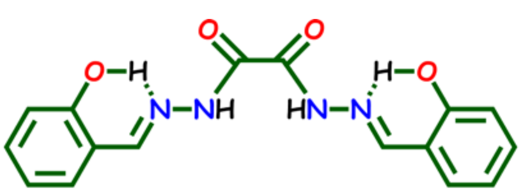	2.0 µM	4.0×10^{3} M^{-1}	New J. Chem., 2016, 40, 8918--8927

	1.24×10^{-3} mM	–	RSC Adv., 2016, 6, 37944–37952
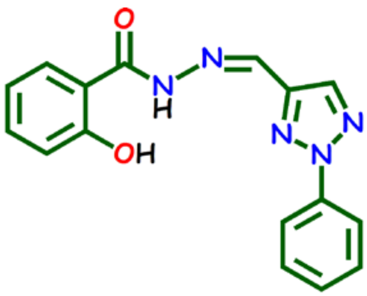	1.2×10^{-8} M	2.4×10^{6} M^{-1}	RSC Adv., 2016,6, 28034-28037
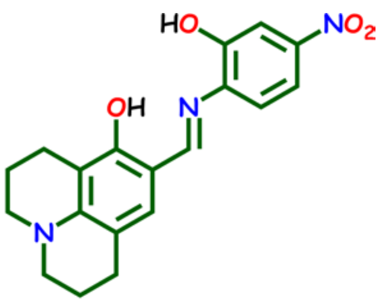	1.5 µM	6.1×10^{3} M^{-1}	New J. Chem., 2016, 40, 7536--7541
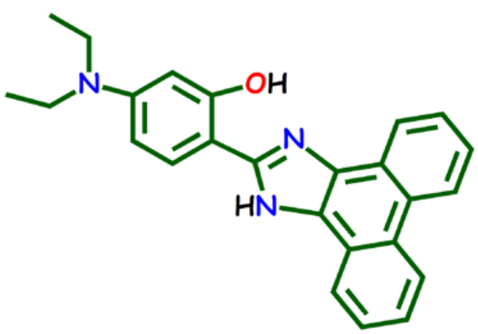	0.5 nM	3.36 $\times10^{5}$ M^{-1}	Inorg. Chem., 2016, 55, 9212
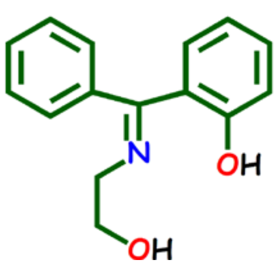	4.61×10^{-7} (M)	10.39 × 10^{4} (M^{-1})	3. Sensors and Actuators B 239 (2017) 1194–1204

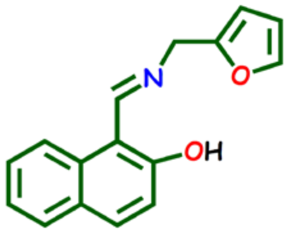	6.03×10^{-7} (M)	0.35×10^{5} (M^{-1})	2. Analyst 137(2012) 3975–3981
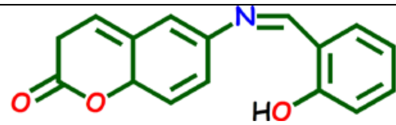	0.5×10^{-6} (M)	7.9×10^{4} (M^{-1})	4. Dalton Trans. 42 (2013) 10198–10207
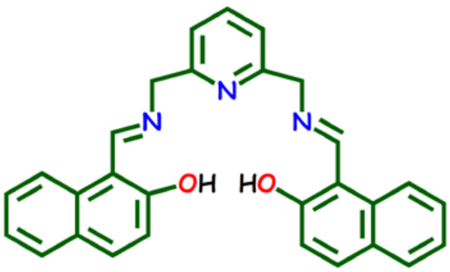	5.6×10^{-6} (M)	3.90×10^{3} (M^{-1})	5. Inorg. Chem. Commun. 35 (2013) 273–275
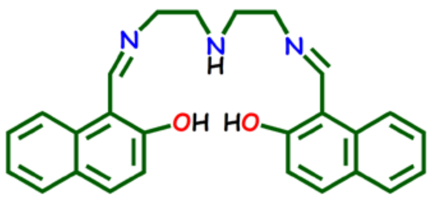	1.0×10^{-7} (M)	2.12×10^{5} (M^{-1})	6. Org. Biomol. Chem. 9 (2011) 5523–5529
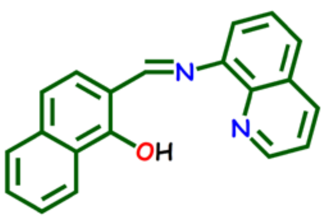	1.1×10^{-5} (M)	3.90×10^{10} (M^{-1})	7. Inorg. Chem. Commun. 33 (2013) 48–51